Lithos 346–347 (2019) 105153

Contents lists available at ScienceDirect

Lithos

journal homepage: www.elsevier.com/locate/lithos

Invited review article

The emerging portrait of an ancient, heterogeneous and continuously evolving mantle plume source

Rita Parai [a,*], Sujoy Mukhopadhyay [b], Jonathan M. Tucker [c], Maria K. Pető [d]

[a] Department of Earth and Planetary Sciences, Washington University in St. Louis, 1 Brookings Dr., St. Louis, MO 63130, United States of America
[b] Department of Earth and Planetary Sciences, University of California Davis, 1 Shields Ave, Davis, United States of America
[c] Department of Terrestrial Magnetism, Carnegie Institution for Science, 5241 Broad Branch R,. NW, Washington, DC 20015, United States of America
[d] Konkoly Observatory, Hungarian Academy of Sciences, 15-17 Konkoly Thege Rd, Budapest 1121, Hungary

ARTICLE INFO

Article history:
Received 27 August 2018
Received in revised form 22 July 2019
Accepted 22 July 2019
Available online 26 July 2019

Keywords:
Plume
Mantle
Noble gases
Mid-ocean ridge basalt
Ocean island basalt
Xenon
Neon
Argon
Helium

ABSTRACT

Heterogeneity in the lithophile isotopic compositions of ocean island basalts (OIBs) has long been ascribed to the incorporation of recycled materials into the plume source. OIB heterogeneity indicates that plumes do not sample a pristine primordial reservoir, but rather sample an inhomogeneous mixture of primordial and recycled material generated by convective processes over Earth history. Here we present a synthesis of new insights into the characteristics and nature of the plume mantle source.

Recent high precision noble gas data demonstrate that the origin of the reservoir supplying noble gases to plumes is fundamentally distinct from that of the mid-ocean ridge basalt (MORB) mantle reservoir: the two reservoirs cannot be related simply by differential degassing or incorporation of recycled atmospheric volatiles. Based on differences observed in the extinct ^{129}I-^{129}Xe system ($t_{1/2}$ of 15.7 Ma), the mantle source supplying noble gases to plumes differentiated from the MORB source within ~100 Ma of the start of the Solar System, and the two sources have not been homogenized by 4.45 Ga of mantle convection. Thus, the ^{129}I-^{129}Xe data require a plume source that has experienced limited direct mixing with the MORB source mantle.

Analysis of mantle source Xe isotopic compositions of plume-influenced samples with primordial He and Ne indicates that the plume source Xe budget is dominated by regassed atmospheric Xe. He and Ne isotopes are not sensitive to regassing due to low overall concentrations of He and Ne in recycled material relative to primordial material. Therefore, plume-influenced samples with primitive He and Ne isotopic compositions do not necessarily reflect sampling of pristine primordial mantle and the lithophile compositions of these samples should not be taken to represent undifferentiated mantle. In addition to recycled atmospheric Xe, the plume mantle source exhibits high ratios of Pu-fission Xe to U-fission Xe. The high proportion of Pu-fission Xe independently confirms a low extent of degassing of the plume source relative to the MORB source.

Heavy noble gases illustrate that the mantle reservoir sampled by plumes is fundamentally distinct from the MORB mantle and reflects ongoing degassing of, and incorporation of recycled material into, an ancient (>4.45 Ga) primordial source. If plumes are derived from large low shear-wave velocity provinces (LLSVPs), then these seismically-imaged structures are ancient and long-lived.

Contents

* Corresponding author.
E-mail address: parai@wustl.edu (R. Parai).

https://doi.org/10.1016/j.lithos.2019.105153
0024-4937/

1. Introduction

Mantle plumes sample a deep Earth reservoir that is chemically distinct from the mantle source of mid-ocean ridge basalts. Plumes are hypothesized to upwell from a boundary layer in the deep Earth, and upon impingement at the base of the lithosphere, drive ocean island or intraplate volcanism (Morgan, 1971; Wilson, 1973). The chemical composition of plume-derived basalts reflects the distinctive history of accretion, differentiation and ongoing modification of the plume mantle source. Accordingly, detailed study of the chemical signatures of plume-derived basalts affords insight into early Earth history, as well as the long-term evolution of Earth's interior in association with solid-state mantle convection and plate tectonics.

Plume-related volcanism samples a mantle source that is more heterogeneous than the mantle source of mid-ocean ridge basalts (MORBs). Among plume-related volcanic samples, isotopic heterogeneity paints a complex picture of deep mantle dynamics. Lithophile long-lived radiogenic isotope signatures (such as $^{87}Sr/^{86}Sr$, $^{143}Nd/^{144}Nd$, $^{206}Pb/^{204}Pb$) have long been noted to vary widely in plume-derived ocean island basalts (e.g., Depaolo and Wasserburg, 1976; Gast et al., 1964; O'Nions et al., 1977; Richard et al., 1976; Tatsumoto, 1978; Zindler et al., 1979; Zindler and Hart, 1986). Much of this heterogeneity has been attributed to the incorporation or entrainment of subducted materials by mantle plumes (e.g., Farley et al., 1992; Hart et al., 1992; Hofmann and White, 1982; Zindler and Hart, 1986). Data from individual ocean island chains form roughly linear subarrays within a broad tetrahedral mantle array in Sr-Nd-Pb isotopic space. These sublinear arrays are thought to reflect mixing between a common plume component (suggested candidates with distinct compositions and origins include the focus zone, "FOZO," Hart et al., 1992; the primitive helium mantle "PHEM," Farley et al., 1992; or the common component, "C," Hanan and Graham, 1996), the depleted mantle (DM) and at least three other endmember components. These endmember components are: enriched mantle I (EM-I), suggested to reflect subcontinental lithospheric mantle, lower continental crust or pelagic sediments (Chauvel et al., 1992; Eisele et al., 2002; Geldmacher et al., 2008; McKenzie and O'Nions, 1983; Weaver et al., 1986; Willbold and Stracke, 2010; Zindler and Hart, 1986); enriched mantle II (EM-II), thought to reflect incorporation of ancient terrigenous sediments (Chauvel et al., 1992; Weaver, 1991); and HIMU ("high μ," where μ is the U/Pb ratio), thought to reflect ancient recycled oceanic crust (Chase, 1981; Chauvel et al., 1992; Hofmann and White, 1982). Carbonate recycling and carbonatitic metasomatism have also been suggested to account for the HIMU signature (Castillo, 2015; Hauri et al., 1993; Nakamura and Tatsumoto, 1988; Weiss et al., 2016). In this framework for understanding ocean island basalt chemical heterogeneity, mantle plumes sample a common reservoir but are variably influenced by subduction-related components at different localities across the globe.

Noble gases are uniquely powerful tools with which to probe the detailed nature of the plume mantle source. Each noble gas has at least one stable, non-radiogenic isotope (referred to as a "primordial" isotope, as budgets of these isotopes were established during accretion), and at least one radiogenic isotope that is produced by nuclear reactions over time. Table 1 categorizes the isotopes of helium (He), neon (Ne), argon (Ar), krypton (Kr) and xenon (Xe). Upon mantle processing by partial melting, all isotopes of the noble gases are lost from mantle reservoirs by degassing. Over time, only the radiogenic noble gas isotopes grow in due to decay of lithophile parent isotopes (Table 1). Therefore, reservoirs that experienced greater extents of processing by partial melting will exhibit higher ratios of radiogenic to primordial isotopes compared to less processed reservoirs. Noble gases are present in such low abundances that their isotopic compositions are strongly sensitive to degassing and subsequent radiogenic, nucleogenic or fissiogenic production, even when radioactive parent nuclides are themselves rare. A diverse set of short-lived (^{129}I, ^{244}Pu) and long-lived (^{235}U, ^{238}U, ^{232}Th, ^{40}K) radioactive nuclides decay to produce isotopes of He, Ne, Ar and Xe, such that noble gas isotopic compositions are sensitive to mantle processing occurring on a wide range of timescales (Fig. 1).

Noble gases are also sensitive to regassing of atmospheric volatiles into the mantle. The noble gas isotopic composition of the atmosphere is distinct from compositions measured in mantle-derived rocks, and based on isotopic variations in mantle-derived samples, recent studies have argued for deep recycling of atmospheric noble gases into the mantle in association with subducting material (Holland and Ballentine, 2006; Kendrick et al., 2011b; Kobayashi et al., 2017; Matsumoto et al., 2001; Mukhopadhyay, 2012; Parai et al., 2012; Pető et al., 2013; Sarda et al., 1999; Sumino et al., 2010; Tucker et al., 2012). Accordingly, noble gases provide a diverse and powerful set of tools that are sensitive to distinct processes occurring on various timescales in Earth history (Fig. 1).

Among the noble gases, He isotopes are the most commonly measured in mantle-derived rocks. Plume He isotopic compositions vary widely relative to MORB He compositions: plume $^4He/^3He$ ranges from ~15,000 to 170,000 (Farley et al., 1992; Graham, 2002; Hilton et al., 1999; Kurz et al., 1983; Kurz and Geist, 1999; Moreira et al., 1999; Stuart et al., 2003), while $^4He/^3He$ typically falls between ~80,000–100,000 for MORBs removed from the influence of plumes ($^3He/^4He$ ratios of ~7–9 R_A, where R_A signifies the atmospheric ratio of 1.39×10^{-6}; Graham, 2002; Graham et al., 1992b; Kurz et al., 1982; Moreira et al., 1998; Tucker et al., 2012). Relatively unradiogenic He isotope ratios ($^4He/^3He < 50{,}000$) in plume-derived samples (e.g., from Hawaii, Iceland, Galapagos and Samoa) are thought to reflect sampling of a mantle source that has experienced less degassing and has thus retained a larger proportion of its primordial ^3He budget relative to the MORB source (e.g., Gonnermann and Mukhopadhyay, 2009; Kellogg and Wasserburg, 1990; Porcelli and Elliott, 2008). Available Ne and Ar isotopic data support this interpretation: plume-derived samples with low $^4He/^3He$ also have relatively low $^{21}Ne/^{22}Ne$ and $^{40}Ar/^{36}Ar$ ratios after correction for atmospheric contamination (Allègre et al., 1987; Allègre et al., 1983; Colin et al., 2015; Graham, 2002; Hiyagon et al., 1992; Honda and Woodhead, 2005; Kaneoka and Takaoka, 1980; Kaneoka et al., 1983; Kurz et al., 2009; Marty et al., 1998; Moreira, 2013; Mukhopadhyay, 2012; Péron et al., 2016; Trieloff et al., 2000; Yokochi and Marty, 2004; see Section 2), consistent with a plume mantle source that has retained a greater portion of its primordial ^{22}Ne and ^{36}Ar budgets relative to the MORB source.

MORB $^4He/^3He$ ratios exhibit less variation than is observed among plume-related samples, which span from unradiogenic ($^4He/^3He$ of ~15,000) to the most radiogenic He measured in mantle-derived rocks ($^4He/^3He > 120{,}000$). High $^4He/^3He$ ratios reflect material that has

Table 1
Noble gas isotopes and dominant production reactions in geological context. Red color indicates isotopes that are generated by nuclear reactions, while isotopes in blue are primordial (i.e., not produced in significant quantities by nuclear reactions). Fissiogenic Kr is rarely significant enough to be resolved, except in U-rich minerals (Hebeda et al., 1987). For each noble gas element, there is at least one primordial isotope and at least one isotope produced by nuclear reactions. Red and blue colors are used throughout the subsequent figures to denote isotopes produced by nuclear reactions over time (red) and primordial isotopes (blue).

Noble gas element	Stable isotopes primordial radiogenic	Dominant production via	Half-life
Helium	^{3}He ^{4}He	^{235}U (α-decay) ^{238}U (α-decay) ^{232}Th (α-decay)	703.8 Myr 4.468 Gyr 14 Gyr
Neon	^{20}Ne ^{21}Ne ^{22}Ne	^{18}O(α,n)^{21}Ne, ^{24}Mg(n,α)^{21}Ne	n/a
Argon	^{36}Ar ^{38}Ar ^{40}Ar	^{40}K (ec)	1.25 Gyr
Krypton	^{78}Kr ^{80}Kr ^{82}Kr ^{83}Kr ^{84}Kr ^{86}Kr	^{244}Pu (sf) ^{238}U (sf)	80.0 Myr 4.468 Gyr
Xenon	^{124}Xe ^{126}Xe ^{128}Xe ^{129}Xe ^{130}Xe ^{131}Xe ^{132}Xe ^{134}Xe ^{136}Xe	^{129}I (β$^-$ decay) ^{244}Pu (sf) ^{238}U (sf)	15.7 Myr 80.0 Myr 4.468 Gyr

ec: electron capture
sf: spontaneous fission

experienced greater extents of degassing, such that radiogenic ingrowth of ^{4}He by α-decay of U and Th strongly impacts the He isotopic composition. The highest plume-related ^{4}He/^{3}He ratios are found at HIMU ocean islands; these signatures are associated with very radiogenic ^{206}Pb/^{204}Pb ratios and are attributed to the incorporation of recycled oceanic crust in the HIMU mantle source (Barfod et al., 1999; Graham et al., 1992a; Hanyu et al., 1999; Hanyu and Kaneoka, 1997; Hilton et al., 2000; Parai et al., 2009; Vance et al., 1989). However, HIMU helium isotopic compositions are less radiogenic than expected for pure recycled components (Graham et al., 1992a; Hanyu and Kaneoka, 1997). Ne isotopic compositions in Cook-Austral Island HIMU basalts and HIMU-type MORBs in the Equatorial Atlantic reveal that the HIMU source must reflect mixing between recycled material and a relatively undegassed plume component (Parai et al., 2009; Tucker et al., 2012). Mixing of recycled material with a less-degassed plume component would explain HIMU helium isotopes and HIMU mixing trends towards a common plume component in the lithophile isotopic data (Hart et al., 1992). Thus, neon isotopes provide an insight into the nature of the HIMU mantle source that is not evident in helium isotopes alone: helium and neon isotopic data reflect a plume mantle source that contains heterogeneous mixtures of primordial and recycled material.

The heavy noble gases (Ne, Ar and Xe) provide a particularly rich record of mantle processing history and must be considered in addition to helium isotopes to study the nature of the plume source mantle. Here we review recent heavy noble gas isotopic data from mantle-derived samples, and discuss the implications for the chemistry and geodynamics of the Earth's deep interior. Based on new high-precision isotopic data, a new portrait emerges of the mantle plume source as an ancient, heterogeneous reservoir that has been continuously modified by convective processes over Earth history.

2. Correcting for *syn*- to post-eruptive atmospheric contamination

Measurements of heavy noble gas isotopic compositions in mantle-derived rocks are affected by pervasive *syn*- to post-eruptive atmospheric contamination (e.g., Moreira et al., 1998; Mukhopadhyay, 2012; Roubinet and Moreira, 2018; Staudacher and Allegre, 1982; Trieloff et al., 2000; Trieloff and Kunz, 2005). Corrections for *syn*- to

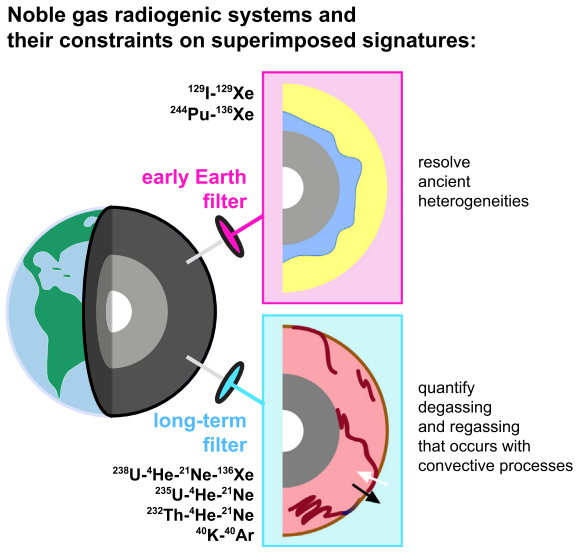

Fig. 1. Viewing the modern Earth through lenses of short- and long-lived radiogenic noble gas isotope systems. The noble gas isotopic composition of the mantle reflects the full integrated history of deep Earth volatile transport and radiogenic production. The short-lived, extinct I-Xe and Pu-Xe systems are sensitive to degassing that occurred during the Hadean, and preserve signatures of ancient mantle heterogeneity. Long-lived extant systems (U-Th-He-Ne-Xe, K-Ar) generate signatures that reflect long-term degassing. Regassing of compositionally distinct atmospheric noble gases also affects the mantle isotopic composition. Thus, a full set of noble gas isotopes measured in mantle-derived samples provides constraints on volatile transport processes on a broad range of timescales, akin to looking at Earth through filters for different time periods.

post-eruptive atmospheric contamination are required to characterize mantle sources, and to accurately interpret their compositions. To this end, step-crushing techniques yield multiple measurements of a single sample in which variable amounts of atmospheric contaminant are released along with mantle gas. In some samples, measured isotopic ratios exhibit well-defined mixing systematics (Figs. 1–4) reflecting this variable mixture of mantle and atmospheric gas. These measured values can be modeled as two-component mixtures between the unknown mantle source isotopic composition and the known atmospheric composition.

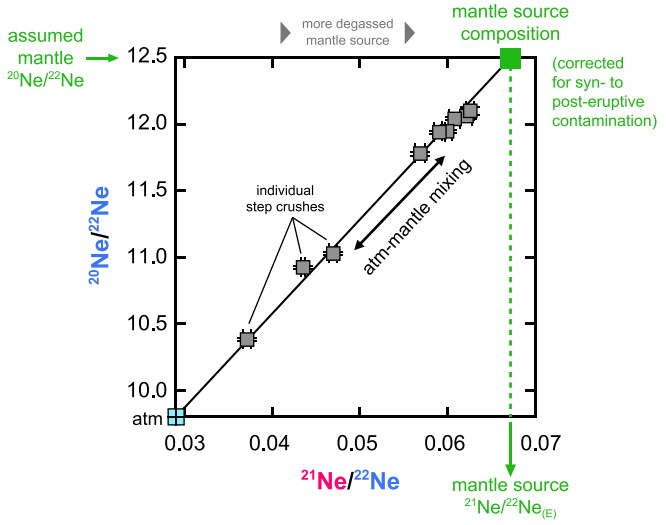

Fig. 2. Ne three isotope diagram. Variable atmospheric contamination of a step-crushed sample. Data are crush-steps from a single MORB (KN162–7 22–14) from the Southwest Indian Ridge (Parai et al., 2012). Axes are the ratio of two primordial isotopes (^{20}Ne/^{22}Ne) vs. the ratio of nucleogenic ^{21}Ne to primordial ^{22}Ne, and mixing is linear in this space. Isotope label colors are defined in Table 1. The step-crush data define a linear array reflecting variable *syn*- to post-eruptive atmospheric contamination of the mantle composition. Assuming a mantle ^{20}Ne/^{22}Ne ratio of 12.5, the mantle source ^{21}Ne/^{22}Ne$_{(E)}$ composition is determined by extrapolation based on the total least-squares line of best fit to the data (green arrows and dashed line). The data array is thus corrected for atmospheric contamination and used to determine the mantle source composition, which allows for comparison between distinct mantle sources. Mantle sources that have experienced more degassing over time develop higher mantle source ^{21}Ne/^{22}Ne$_{(E)}$ compositions and shallower slopes in this diagram.

2.1. Correction for atmospheric contamination of Ne isotopes

There are three isotopes of neon: ^{20}Ne, ^{21}Ne and ^{22}Ne. Of these, ^{20,22}Ne are primordial and ^{21}Ne is produced by nuclear reactions, e.g., ^{18}O(α,n)^{21}Ne and ^{24}Mg(n,α)^{21}Ne (Table 1). Mixing in ^{20}Ne/^{22}Ne vs. ^{21}Ne/^{22}Ne isotopic space is linear. High-precision neon isotopic data produced by step-crushing of mantle-derived samples exhibit linear mixing systematics in Ne three-isotope space, with the atmospheric Ne composition constituting one mixing endmember (Fig. 2). To correct for *syn*- to post-eruptive atmospheric contamination, we assume a mantle source ^{20}Ne/^{22}Ne composition, and the mantle source

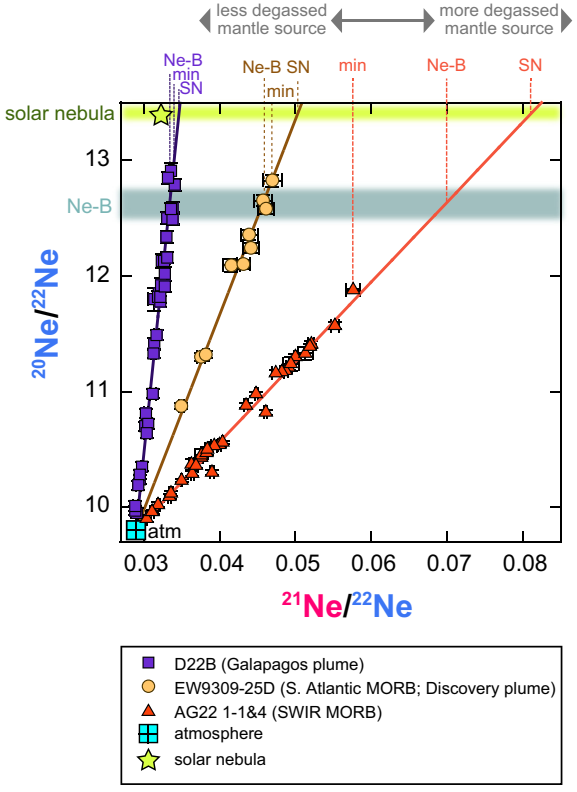

Fig. 3. Mantle source Ne compositions for distinct plume and MORB mantle sources given different mantle ^{20}Ne/^{22}Ne models. Data are crush steps from Galapagos sample D22B (Péron et al., 2016), a plume-influenced MORB from the S. Atlantic Ridge (EW9309-25D; Williams and Mukhopadhyay, 2019), and Southwest Indian Ridge MORB (AG22 1–1&4; Parai et al. (2012). The ^{21}Ne/^{22}Ne ratio of the mantle source corrected for atmospheric contamination is determined by fitting a line to the data for a single sample, and then extrapolating to a model primordial mantle ^{20}Ne/^{22}Ne value (Fig. 2). The highest measured crush step value represents the minimum mantle source ^{21}Ne/^{22}Ne composition (min); the composition prior to atmospheric contamination was at least this high. Mantle source ^{21}Ne/^{22}Ne$_{(E)}$ values reflecting a Ne-B or solar nebular (SN) primordial mantle Ne model are indicated for comparison. Even though the absolute ^{21}Ne/^{22}Ne$_{(E)}$ value changes based on the primordial Ne model, relative variations among plume-influenced samples and MORBs are not sensitive to the model. The slopes of the plume-atmosphere mixing arrays are sufficiently steep that uncertainty in the mantle endmember ^{20}Ne/^{22}Ne (Ne-B vs. solar nebular; Moreira and Charnoz, 2016; Heber et al., 2012) does not affect relative ^{21}Ne/^{22}Ne$_{(E)}$ systematics between plumes and MORBs: even if the plume-influenced samples are extrapolated to the solar nebular value and the MORB is extrapolated to the Ne-B value, ^{21}Ne/^{22}Ne$_{(E)}$ in the plume-influenced samples is lower, reflecting less-degassed mantle sources. We note that the Galapagos data reflect a mantle source that has experienced very little degassing, as the slope is nearly as steep as a solar nebula-atmosphere mixing line.

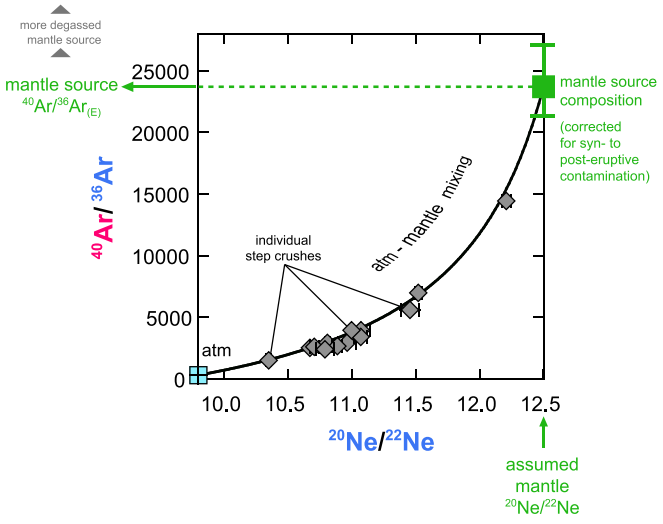

Fig. 4. Ne-Ar hyperbolic mixing arrays showing variable atmospheric contamination of a step-crushed sample. Data are crush steps from Southwest Indian Ridge MORB AII107–6 57–5 from Parai et al. (2012). The axes are the ratio of radiogenic ^{40}Ar to primordial ^{36}Ar vs. primordial Ne isotopes. Assuming a mantle primordial Ne isotopic composition, the mantle source $^{40}Ar/^{36}Ar_{(E)}$ ratio is determined by extrapolation based on the total least squares hyperbolic best fit to the data (green arrows and dashed line). Correcting for atmospheric contamination allows for comparison between distinct mantle sources. Higher mantle source $^{40}Ar/^{36}Ar_{(E)}$ ratios may reflect a reservoir that has experienced more degassing.

$^{21}Ne/^{22}Ne$ is determined by linear fitting of the data and extrapolation to the mantle source $^{20}Ne/^{22}Ne$ ratio (Fig. 2; $^{21}Ne/^{22}Ne_{(E)}$, where E stands for extrapolated). Degassing generates high $(U + Th)/^{22}Ne$ ratios, such that a more-degassed mantle reservoir would develop high mantle source $^{21}Ne/^{22}Ne_{(E)}$ over time. As radioactive decay of U and Th drive the nuclear reactions that produce ^{21}Ne, radiogenic ^{4}He and nucleogenic ^{21}Ne production are directly linked.

The best fit line may be determined by total least squares fitting with correlated errors (York, 1969; York et al., 2004). We note that for MORB samples, corrections are commonly made to a mantle source $^{20}Ne/^{22}Ne$ of 12.5 (Moreira, 2013; Moreira et al., 1995; Moreira et al., 1998; Parai et al., 2012), consistent with primordial mantle neon reflecting the Ne-B component (e.g., Ballentine et al., 2005; Péron et al., 2017; Raquin et al., 2008; Trieloff et al., 2000). Although the value of the Ne-B $^{20}Ne/^{22}Ne$ ratio has been debated and may be as high as 12.7 (Moreira and Charnoz, 2016; Péron et al., 2018a), analyses of plume-derived samples have yielded $^{20}Ne/^{22}Ne$ measurements greater than and resolved from 12.7: e.g., step-crushed samples from Iceland have $^{20}Ne/^{22}Ne$ up to 12.88 ± 0.06 (1σ) (Mukhopadhyay, 2012), step-crushed samples from Galapagos have $^{20}Ne/^{22}Ne$ up to 12.91 ± 0.07 (1σ) (Péron et al., 2016), and step-crushed samples from the Kola peninsula exhibit $^{20}Ne/^{22}Ne$ up to 13.04 ± 0.20 (1σ) (Yokochi and Marty, 2004). Plume-influenced MORBs from the S. Atlantic also exhibit measured $^{20}Ne/^{22}Ne$ ratios up to 13.03 ± 0.04 (2σ; Williams and Mukhopadhyay, 2019), well-resolved from the high end of estimates of the Ne-B composition. Measured $^{20}Ne/^{22}Ne$ ratios greater than (and resolved from) the Ne-B value are most consistent with a plume source primordial Ne budget derived from solar nebula with $^{20}Ne/^{22}Ne$ of ~13.4 (Heber et al., 2012). In this case, the highest measured $^{20}Ne/^{22}Ne$ ratios (<13.1) may reflect some *syn*- to post-eruptive atmospheric contamination, and the pure mantle endmember (with nebular $^{20}Ne/^{22}Ne$) has not yet been directly measured. Alternatively, the MORB and plume mantle sources incorporated some limited amount of chondritic Ne during accretion or recycled atmospheric Ne with low $^{20}Ne/^{22}Ne$, such that the mantle source $^{20}Ne/^{22}Ne$ ratios are lower than 13.4, and potentially variable among mantle sources (Williams and Mukhopadhyay, 2019).

We note that uncertainties regarding the mantle $^{20}Ne/^{22}Ne$ ratio and its origins have a limited impact on the interpretation of $^{21}Ne/^{22}Ne$ variations among various mantle sources. Data from mid-ocean ridge basalts form mixing arrays with relatively shallow slopes in Ne three-isotope space, while plume-derived samples are characterized by steeper slopes (Farley and Poreda, 1993; Graham, 2002; Honda et al., 1991; Kurz et al., 2009; Moreira, 2013; Moreira et al., 1998; Mukhopadhyay, 2012; Parai et al., 2012; Pető et al., 2013; Poreda and Farley, 1992; Trieloff et al., 2000; Tucker et al., 2012). If the MORB mantle source $^{20}Ne/^{22}Ne$ is >12.5, then the differences between MORB and plume mantle source $^{21}Ne/^{22}Ne_{(E)}$ ratios would be slightly larger than presently discussed (Fig. 3). For plume-influenced samples, the air-mantle mixing slopes in ^{20}Ne -^{21}Ne -^{22}Ne isotopic space are sufficiently steep that extrapolation to a mantle source $^{20}Ne/^{22}Ne$ of 13.4 rather than ~12.8–13.1 would not change the broad systematics between MORB and plume sources (Fig. 3).

2.2. Correction for atmospheric contamination of Ar isotopes

There are three isotopes of argon: $^{36,38}Ar$ are primordial, while ^{40}Ar is produced by electron capture on ^{40}K (Table 1). Variations in $^{40}Ar/^{36}Ar$ measured by step-crushing of a single sample reflect variable mixing between a mantle source and the atmospheric composition. However, $^{38}Ar/^{36}Ar$ ratios are not resolved from the atmospheric composition (Mukhopadhyay, 2012; Raquin and Moreira, 2009). Therefore, mixing systematics are sought in $^{40}Ar/^{36}Ar$ vs. $^{20}Ne/^{22}Ne$ space rather than argon three-isotope space. Mixing in Ne-Ar isotope space is hyperbolic; a method to correct for *syn*- to post-eruptive atmospheric contamination using orthogonal least squares fitting for two-component hyperbolic mixing is described by Parai et al. (2012) and an algorithm is given in the appendix to Parai (2014). Based on mixing systematics evident in step-crushed mantle-derived samples, the mantle source $^{40}Ar/^{36}Ar_{(E)}$ composition is determined by extrapolation to a fixed $^{20}Ne/^{22}Ne$ value. The curvature of a two-component mixing hyperbola depends on the $^{36}Ar/^{22}Ne$ ratios of the two endmembers, and air-mantle mixing hyperbolas tend to be concave-up in $^{40}Ar/^{36}Ar$ vs. $^{20}Ne/^{22}Ne$ space (Fig. 4). Depending on the curvature of the hyperbola, extrapolation to a mantle source $^{20}Ne/^{22}Ne$ ratio higher than 12.5 may translate to a significantly higher mantle source $^{40}Ar/^{36}Ar$. However, we note that for some MORB samples with well-defined hyperbolic mixing, best fit hyperbolae asymptote with respect to the y-axis at $^{20}Ne/^{22}Ne$ ratios lower than 13.4, so the mantle source $^{20}Ne/^{22}Ne$ ratios for these samples must be below this value (Fig. 4).

2.3. Correction for atmospheric contamination of Xe isotopes

There are nine isotopes of xenon: $^{124,126,128,130}Xe$ are primordial, ^{129}Xe is radiogenic, and $^{131,132,134,136}Xe$ are fissiogenic. ^{124}Xe and ^{126}Xe are the lowest in abundance, and have only been measured with sufficient precision to resolve a mantle signature from atmosphere in a select few samples: well gases and the gas-rich popping rock 2ΠD43 (Caffee et al., 1999; Caracausi et al., 2016; Holland et al., 2009; Holland and Ballentine, 2006; Péron et al., 2018b). ^{128}Xe is also low in abundance, and $^{128}Xe/^{130}Xe$ ratios measured in mantle-derived rocks are generally not sufficiently precise or distinct from the atmospheric composition to use to correct other ^{130}Xe-normalized ratios for atmospheric contamination through linear fitting. Therefore, hyperbolic mixing systematics are also sought in Ne-Xe or Ar-Xe isotopic space.

Mantle source $^{129}Xe/^{130}Xe_{(E)}$ and $^{129,130,131,134,136}Xe/^{132}Xe_{(E)}$ isotopic compositions are typical isotope ratios of interest for mantle-derived samples. To determine the mantle source $^{129}Xe/^{130}Xe_{(E)}$ ratio, previous studies have applied the same hyperbolic fitting methods as mentioned in Section 2.2 for $^{129}Xe/^{130}Xe$ vs. $^{20}Ne/^{22}Ne$ and $^{129}Xe/^{130}Xe$ vs. $^{40}Ar/^{36}Ar$ (Fig. 5). In favorable cases, $^{130}Xe/^{22}Ne$ and $^{130}Xe/^{36}Ar$ ratios in the mantle and atmospheric contaminant are such that hyperbolic mixing arrays asymptote with respect to the Ne or Ar axis. This means that extrapolated mantle source $^{129}Xe/^{130}Xe_{(E)}$ values are not very sensitive to uncertainty in the mantle endmember $^{20}Ne/^{22}Ne$ or $^{40}Ar/^{36}Ar_{(E)}$

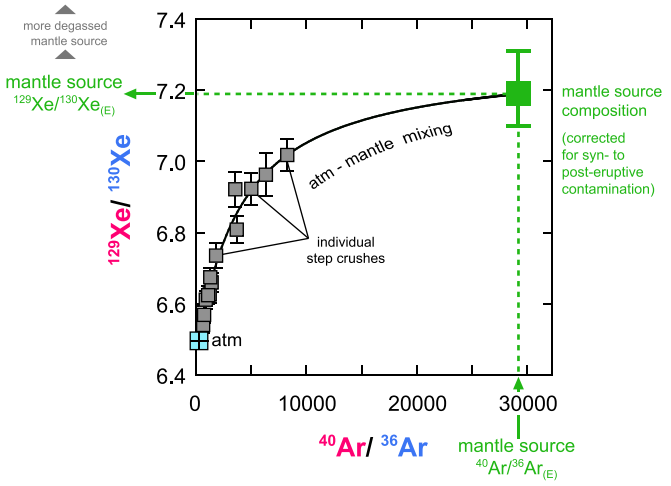

Fig. 5. Ar-Xe hyperbolic mixing arrays showing variable atmospheric contamination of a step-crushed sample. Data are crush steps from Southwest Indian Ridge MORB AG22–13-1 from Parai et al. (2012). The axes are the ratio of radiogenic ^{129}Xe to primordial ^{130}Xe vs. ^{40}Ar/^{36}Ar. A similar plot may be made with ^{20}Ne/^{22}Ne on the x-axis. Based on the mantle source ^{40}Ar/^{36}Ar$_{(E)}$ ratio determined using Ne-Ar systematics, the mantle source ^{129}Xe/^{130}Xe$_{(E)}$ ratio is determined by extrapolation based on the total least squares hyperbolic best fit to the data (green arrows and dashed line). Many samples yield mixing hyperbolae that are concave down in this isotope space, which reduces the sensitivity of ^{129}Xe/^{130}Xe$_{(E)}$ to the mantle source ^{40}Ar/^{36}Ar$_{(E)}$ composition as the hyperbola asymptotes with respect to the x-axis. Correcting for atmospheric contamination allows for comparison between distinct mantle sources. Higher mantle source ^{129}Xe/^{130}Xe$_{(E)}$ ratios reflect a reservoir that was characterized by high I/Xe during the lifetime of ^{129}I (the first ~100 Myr of Earth history).

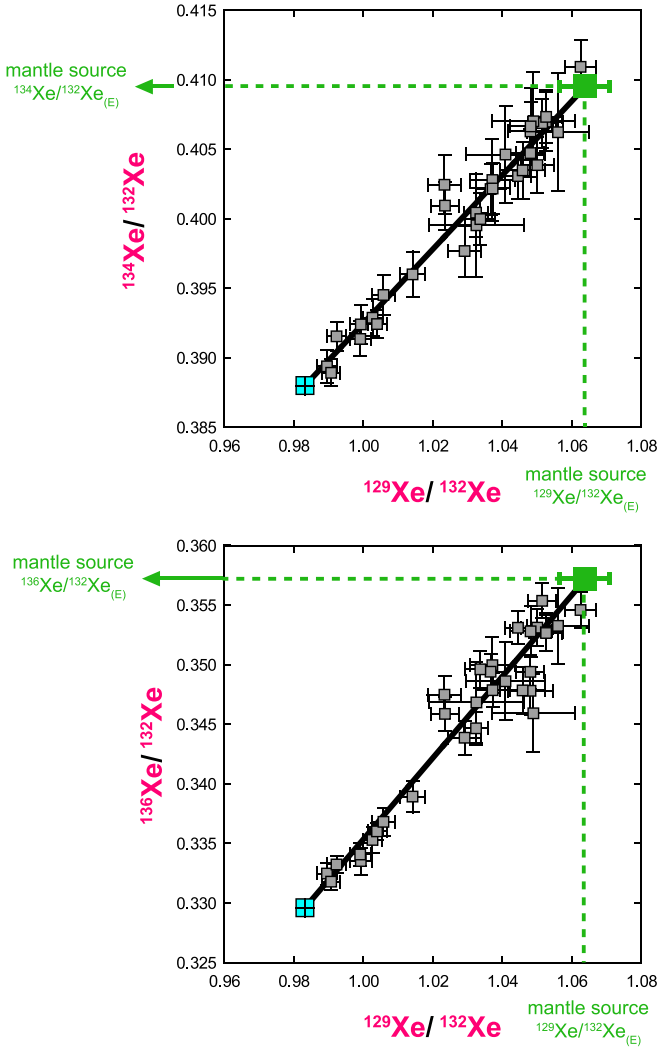

Fig. 6. Xe fission isotope diagrams showing variable atmospheric contamination of step-crushed samples. Data are crush steps from Southwest Indian Ridge MORB Eastern Orthogonal Supersegment MORBs from Parai and Mukhopadhyay (2015). The mantle source ^{129}Xe/^{132}Xe$_{(E)}$ composition determined by Ar-Xe fitting (analogous to Fig. 5) is used to determined mantle source compositions for other ^{132}Xe-normalized isotope ratios based on the total least squares best fit of the data (green arrows and dashed lines). This mantle source composition is then used to determine the proportions of mantle source Xe from initial Xe, regassed atmospheric Xe, Pu-fission Xe and U-fission Xe.

composition, and for clean hyperbolic data arrays, there is an upper limit to the mantle source ^{129}Xe/^{130}Xe$_{(E)}$ corresponding to the asymptote of the hyperbola. We note that Xe-Ar systematics tend to be cleaner than Xe-Ne systematics: their best fit hyperbolae have lower uncertainties that better constrain the mantle source ^{129}Xe/^{130}Xe$_{(E)}$ isotope composition.

Best-fit hyperbolae in ^{129}Xe/^{132}Xe vs. ^{40}Ar/^{36}Ar isotopic space are used to determine mantle source ^{129}Xe/^{132}Xe$_{(E)}$. Ratios normalized to ^{132}Xe rather than ^{130}Xe are useful for computations to determine the proportions of mantle Xe derived from different sources and processes (Section 3), as ^{130}Xe is not produced by fission of U or Pu (Table 1) and ^{130}Xe-normalized ratios of fission components are thus infinite. Furthermore, ^{132}Xe is relatively abundant and using ^{132}Xe-normalized ratios decreases the propagated error relative to ^{130}Xe-normalized ratios. After determining the mantle source ^{129}Xe/^{132}Xe$_{(E)}$ based on Ne-Xe and Ar-Xe systematics, the rest of the mantle source ^{132}Xe-normalized isotopic compositions may be determined by linear least squares fitting with correlated errors (York, 1969; York et al., 2004) and extrapolation to the mantle ^{129}Xe/^{132}Xe$_{(E)}$ composition (Fig. 6; Mukhopadhyay, 2012; Parai and Mukhopadhyay, 2015). Uncertainty in the mantle source ^{129}Xe/^{132}Xe$_{(E)}$ is propagated to the other mantle source ^{132}Xe-normalized Xe isotopic ratios.

3. Linear least squares modeling of the mantle Xe isotopic composition

The present-day ^{131,132,134,136}Xe inventory in mantle sources can be modeled as a mixture of four components: (1) an initial Xe budget, likely chondritic in composition (Caracausi et al., 2016); (2) atmosphere-derived Xe transported and incorporated into the mantle ("regassed" atmospheric Xe); (3) Pu-fission Xe produced within the first ~500 Myr of Earth history and retained in the mantle; and (4) U-fission Xe retained in the mantle. ^{244}Pu and ^{238}U each produce fission ^{131,132,134,136}Xe in characteristic proportions that are distinct from the composition of Earth's atmosphere, of primitive materials such as carbonaceous chondrites, and of each other. Accordingly, the Xe isotopic composition of the mantle source today may be described with four mixing equations of the form:

$$x_{init}\left(\frac{^{\zeta}Xe}{^{132}Xe}\right)_{init} + x_{atm}\left(\frac{^{\zeta}Xe}{^{132}Xe}\right)_{atm} + x_{Pu}\left(\frac{^{\zeta}Xe}{^{132}Xe}\right)_{Pu} + x_U + \left(\frac{^{\zeta}Xe}{^{132}Xe}\right)_{U} = \left(\frac{^{\zeta}Xe}{^{132}Xe}\right)_{mantle} \quad (1)$$

where $\zeta = ^{130}$Xe, ^{131}Xe, ^{134}Xe and ^{136}Xe; x is the molar mixing proportion of ^{132}Xe; *init* designates the initial mantle composition, discussed here as average carbonaceous chondrite (AVCC); *atm* designates recycled atmospheric Xe; *Pu* designates Pu-fission Xe; and *U* designates U-fission Xe. Component Xe isotopic ratios and references are given in Table 2. The ^{132}Xe mixing proportions sum to 1:

$$x_{init} + x_{atm} + x_{Pu} + x_U = 1 \quad (2)$$

To determine the proportions of mantle ^{132}Xe derived from each of these four components, we use a linear least squares approach to

Table 2
Xenon component compositions.

Component	$^{130}Xe/^{132}Xe$	$^{131}Xe/^{132}Xe$	$^{134}Xe/^{132}Xe$	$^{136}Xe/^{132}Xe$
Atmosphere[a]	0.1513	0.7895	0.3880	0.3296
AVCC[b]	0.1626	0.8200	0.3836	0.3233
Pu-fission[c]	0	0.2777	1.0413	1.1198
U-fission[d]	0	0.1449	1.4370	1.7375

[a] Basford et al. (1973).
[b] Average carbonaceous chondrite; Pepin (1991, 2000).
[c] Error-weighted average of data from Alexander et al. (1971), Lewis (1975) and Hudson et al. (1989).
[d] Error-weighted average of data from Wetherill (1953), Hebeda et al. (1987), Eikenberg et al. (1993) and Ragettli et al. (1994).

solve this over-determined system (see Mukhopadhyay, 2012; Parai and Mukhopadhyay, 2015 for a detailed description of numerical methods). Based on such analysis, we may constrain a set of important quantities: the fraction of mantle ^{132}Xe derived from injection of atmospheric Xe into the mantle beyond depths of arc magma generation (referred to as "regassing," Section 4), the ratio of ^{129}I-derived radiogenic ^{129}Xe to Pu-fission derived ^{136}Xe ($^{129}Xe^*/^{136}Xe_{Pu}$) (Section 6), and the ratio of Pu-fission ^{136}Xe to total fission ^{136}Xe ($^{136}Xe_{Pu}/(^{136}Xe_{Pu} + ^{136}Xe_U)$) (Section 7). Fig. 7 shows the fraction of ^{132}Xe derived from each of the four mixing components for MORB and plume mantle sources. Parai and Mukhopadhyay (2015) provide a catalog of linear least squares results from plume and MORB mantle-derived samples, and results using AVCC as the initial mantle component are given in Table 3.

We emphasize that the mantle source Xe compositions have already been explicitly corrected for post- to *syn*- eruptive atmospheric contamination of Xe based on correlations with $^{20}Ne/^{22}Ne$ and $^{40}Ar/^{36}Ar$ prior to applying the linear least squares treatment (Section 2.3). Bulk contamination with atmospheric gas affects measured Ne, Ar and Xe isotopic compositions; after correcting to a mantle $^{20}Ne/^{22}Ne$ value of 12.5 for MORB sources (Parai et al., 2012; Tucker et al., 2012) or higher for plume sources (Mukhopadhyay, 2012; Pető et al., 2013), we interpret any remaining signature of atmospheric Xe as due to regassing. If we were to extrapolate to a higher mantle $^{20}Ne/^{22}Ne$ value in correcting for *syn*- to post-eruptive contamination, for most samples the impact on the mantle source Xe isotopic composition would be minimal due to the favorable curvature of hyperbolic mixtures in Ar-Xe space (Fig. 5). Data from plume-influenced locations (Mukhopadhyay, 2012; Pető et al., 2013) and mid-ocean ridge locations (Parai et al., 2012; Parai and Mukhopadhyay, 2015; Tucker et al., 2012) have been analyzed as described here for their heavy noble gas isotope systematics, and a review of the main insights from these studies is presented below.

4. Isotopic evidence for recycling of atmospheric heavy noble gases into plume and MORB mantle sources

Subducting plates carry atmospheric noble gases dissolved in pore fluids and trapped in minerals within sediments, altered oceanic crust and serpentinized lithospheric mantle (Chavrit et al., 2016; Kendrick et al., 2011b; Kendrick et al., 2013; Kendrick et al., 2018; Kobayashi et al., 2017; Kumagai et al., 2003; Matsuda and Matsubara, 1989; Matsuda and Nagao, 1986; Matsumoto et al., 2001; Podosek et al., 1980; Sumino et al., 2010). High pressures and temperatures at subduction zones were long thought to inhibit the recycling of noble gases into the deep mantle (Moreira and Raquin, 2007; Staudacher and Allègre, 1988). As subducting plates are subjected to increased pressures and temperatures, expulsion of pore fluids and breakdown of hydrous mineral phases removes atmospheric noble gases from downgoing slabs. However, heavy noble gas systematics recently determined in mantle-derived samples reflect the incorporation of modern atmosphere into the mantle, such that atmospheric heavy noble gases must not be completely removed from downgoing slabs. Based on heavy noble gas

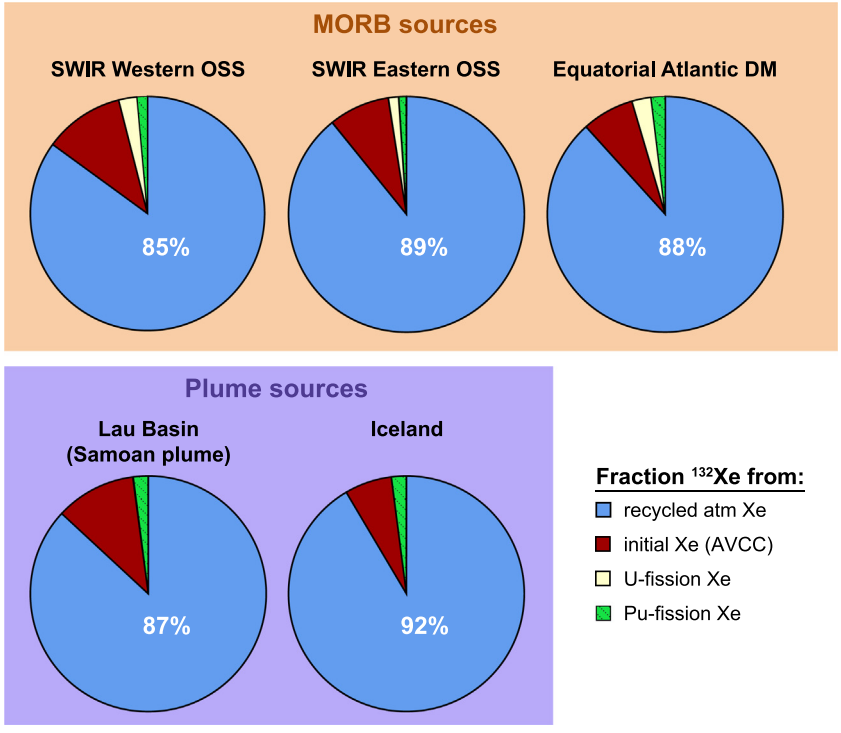

Fig. 7. Results of linear least squares component analysis. Both MORB and plume source Xe budgets are dominated by regassed atmospheric Xe. The initial Xe component is taken to be average carbonaceous chondrite (AVCC) but broad systematics are not dependent on the choice of initial component composition. Full results and uncertainties are given in Table 3 and in Parai and Mukhopadhyay (2015). Proportions of fission Xe from Pu-fission and U-fission vary between MORB and plume mantle sources, with Pu-fission Xe dominating in plume mantle sources (see Fig. 12).

Table 3
Compiled results of Xe from linear least squares mixing computation, using AVCC as the initial mantle Xe composition.

		Initial mantle	Recycled atmosphere	Pu-fission	U-fission	$\frac{^{129}Xe*}{^{136}Xe_{Pu}}$	$\frac{^{136}Xe_{Pu}}{^{136}Xe_{Pu}+^{136}Xe_{U}}$
SWIR Western Orthogonal Supersegment Parai and Mukhopadhyay (2015)	Median	0.110	0.850	0.014	0.025	10.8	0.27
	+1σ	0.069	0.068	0.011	0.006	39.4	0.20
	−1σ	0.063	0.074	0.011	0.006	4.8	0.21
SWIR Eastern Orthogonal Supersegment Parai and Mukhopadhyay (2015)	Median	0.083	0.892	0.011	0.014	8.3	0.32
	+1σ	0.040	0.043	0.007	0.004	14.6	0.19
	−1σ	0.040	0.043	0.007	0.004	3.2	0.20
Equatorial Atlantic Depleted Mantle (Tucker et al., 2012)	Median	0.071	0.883	0.019	0.026	8.1	0.32
	+1σ	0.064	0.069	0.011	0.005	8.3	0.17
	−1σ	0.064	0.069	0.010	0.006	2.9	0.16
Bravo Dome Well Gas (Holland and Ballentine, 2006)	Median	0.095	0.878	0.017	0.010	8.8	0.27
	+1σ	0.037	0.040	0.003	0.006	14.0	0.16
	−1σ	0.037	0.040	0.003	0.006	3.3	0.16
Harding County Well Gas (Caffee et al., 1999)	Median	0.119	0.852	0.011	0.018	7.7	0.28
	+1σ	0.016	0.017	0.003	0.002	2.5	0.07
	−1σ	0.016	0.017	0.003	0.002	1.5	0.07
Lau Basin, Samoan plume - NLD27 (Pető et al., 2013)	Median	0.110	0.869	0.020	0.001	2.9	0.95
	+1σ	0.011	0.030	0.001	0.003	1.0	0.04
	−1σ	0.027	0.012	0.005	0.001	0.2	0.23
Iceland plume – DICE (Mukhopadhyay, 2012)	Median	0.065	0.915	0.020	0.0001	2.8	0.99
	+1σ	0.012	0.024	0.001	0.003	0.7	0.01
	−1σ	0.022	0.012	0.004	0	0.1	0.19
MORB mantle average	Median					8.2	0.31
	+1σ					2.0	0.11
	−1σ					1.3	0.11
Plume-influenced average	Median					2.9	0.97
	+1σ					0.4	0.02
	−1σ					0.1	0.11

For skewed distributions, +1σ and −1σ give 68% confidence limits.

data measured in continental well gases, Holland and Ballentine (2006) noted that MORB source mantle heavy noble gas elemental abundance patterns closely resembled air-saturated seawater. Ratios of primordial isotopes of the different noble gases measured in well gases are distinct from potential precursor components such as solar wind: $^{84}Kr/^{36}Ar$ and $^{130}Xe/^{36}Ar$ ratios in both well gases and the North Atlantic "popping rock" MORB sample (2ΠD43; Moreira et al., 1998) are elevated with respect to the solar composition. These elemental abundance patterns may be affected by fractionation due to degassing; however, the good agreement between Bravo Dome well gas and 2ΠD43 was argued to indicate minimal fractionation of the mantle source elemental patterns by shallow degassing processes. Rather, Holland and Ballentine (2006) suggested that incorporation of atmospheric noble gases via seawater subduction explained the mantle noble gas elemental abundance patterns. This interpretation is supported by observations of seawater-derived volatiles persisting in slabs to depths of at least ~100 km (e.g., Kendrick et al., 2011a; Matsumoto et al., 2001; Sumino et al., 2010), and is further supported by detailed examination of Ar and Xe isotopic compositions of mantle-derived samples, which indicates that atmospheric Ar and Xe are recycled into the mantle.

4.1. Recycled atmospheric argon and xenon in the MORB mantle

Broad co-variations among radiogenic noble gas isotope ratios are evident among mantle-derived samples (Holland and Ballentine, 2006; Moreira, 2013; Mukhopadhyay, 2012; Parai et al., 2012; Pető et al., 2013; Tucker et al., 2012). Low $^{4}He/^{3}He$ in plume samples are associated with relatively low $^{21}Ne/^{22}Ne$ (Moreira, 2013). In samples from Iceland and from the Lau Basin, where the Samoan plume influences the mantle source, low $^{4}He/^{3}He$ is also paired with low $^{40}Ar/^{36}Ar$ (Fig. 8; Mukhopadhyay, 2012; Pető et al., 2013), consistent with a less-degassed mantle source of plumes. These samples are also characterized by relatively low $^{129}Xe/^{130}Xe$, which indicates a low I/Xe ratio in the plume source that must be inherited early in Earth history (Mukhopadhyay, 2012; Pető et al., 2013). In contrast, MORB samples from the North Atlantic and Equatorial Atlantic exhibit relatively high $^{4}He/^{3}He$, $^{21}Ne/^{22}Ne$, $^{40}Ar/^{36}Ar$ and $^{129}Xe/^{130}Xe$ (Moreira et al., 1998; Péron et al., 2019; Péron and Moreira, 2018; Stroncik and Niedermann, 2016; Tucker et al., 2012). These MORBs sample a mantle source that is more degassed than the mantle source of plumes (Fig. 8).

A suite of MORB samples from the Southwest Indian Ridge (SWIR) between 16°E and 25°E reveal MORB source mantle heterogeneity in $^{40}Ar/^{36}Ar$ and $^{129}Xe/^{130}Xe$ (Parai et al., 2012). Step crush data were obtained from samples from the Orthogonal Supersegment, a 600 km stretch of the SWIR removed from the influence of mantle plumes (the nearest plume being Bouvet, >500 km east of the Orthogonal Supersegment). As was done for the plume and MORB samples discussed above, SWIR step crush data were corrected for post- to *syn*-eruptive atmospheric contamination using the methods described in Section 2. After correction for atmospheric contamination (mantle source isotopic compositions corresponding to a $^{20}Ne/^{22}Ne$ ratio of 12.5), the $^{40}Ar/^{36}Ar$ and $^{129}Xe/^{130}Xe$ isotopic compositions of SWIR Orthogonal Supersegment MORB source mantle were found to vary widely. SWIR Orthogonal Supersegment $^{40}Ar/^{36}Ar$ ratios vary from ~20,000 to ~50,000, representing ~70% of the total variation determined in mantle source Ar isotopes (Fig. 8b; Moreira et al., 1998; Mukhopadhyay, 2012; Parai et al., 2012; Péron et al., 2016; Pető et al., 2013; Tucker et al., 2012). SWIR $^{129}Xe/^{130}Xe$ ratios vary from 7.1 to 7.8, representing ~80% of the total mantle source variation determined in $^{129}Xe/^{130}Xe$ ratios (Fig. 8c). Most notably, these variations in radiogenic Ar and Xe isotope ratios at the SWIR are associated with very limited variation in $^{4}He/^{3}He$ or $^{21}Ne/^{22}Ne_{(E)}$ ratios (Parai et al., 2012). In He-Ne isotopic space (Fig. 8a), variations among mantle sources are entirely consistent with differential degassing (see Moreira, 2013 for a comprehensive review of He-Ne systematics in mantle-derived samples). In He-Ar and He-Xe space, MORB heterogeneity suggests another process affects Ar and Xe isotopic compositions. In particular, the Eastern Orthogonal Supersegment samples exhibit low $^{40}Ar/^{36}Ar$ and low $^{129}Xe/^{130}Xe$, similar to the mantle source values determined for plume-derived samples, while their $^{4}He/^{3}He$ and $^{21}Ne/^{22}Ne$ compositions are similar to other MORB sources (Fig. 8). Since the Bouvet plume influences some SWIR MORBs, plume influence was investigated

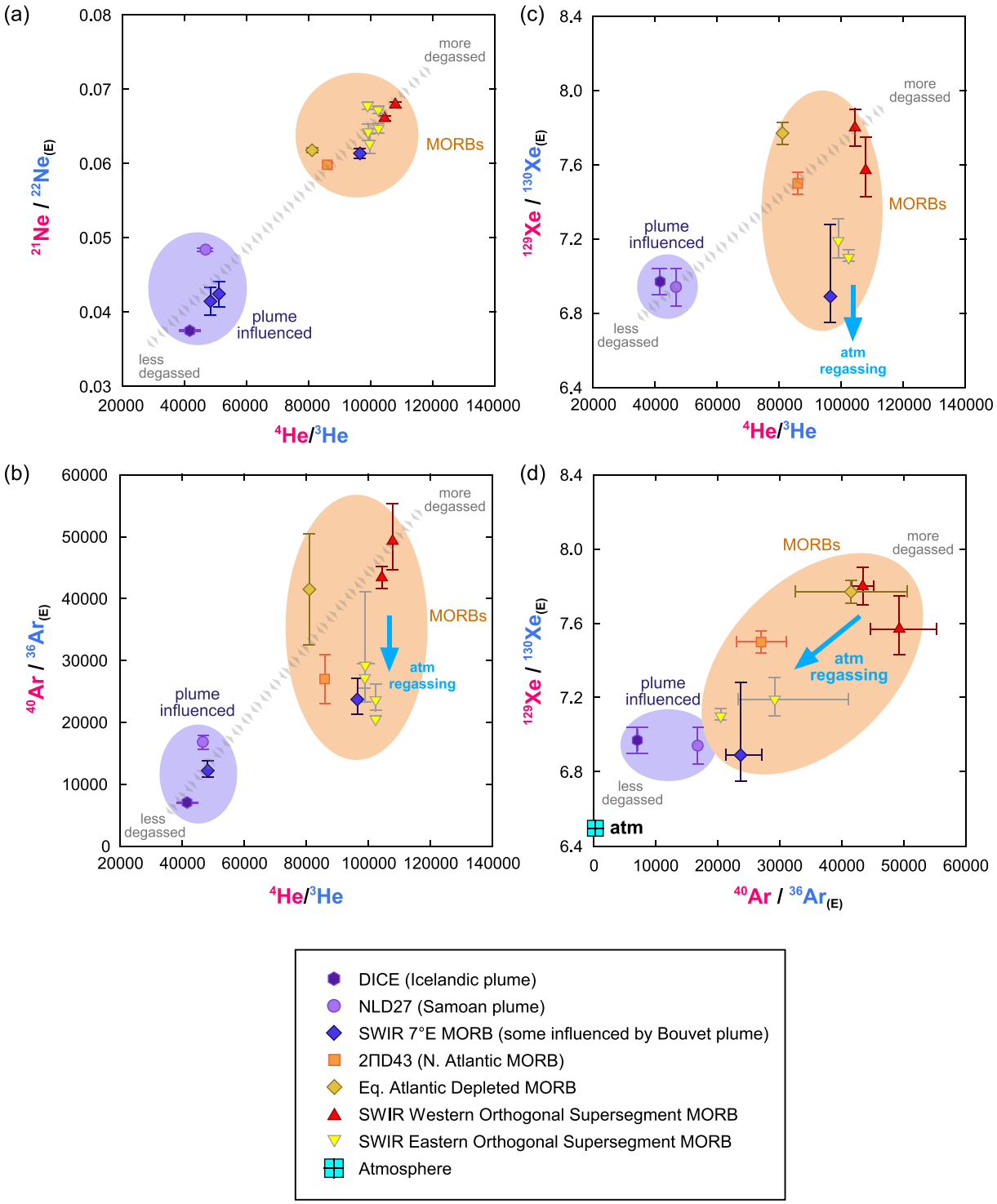

Fig. 8. Isotope ratio plots showing plume mantle and MORB mantle compositions. Each axis shows the ratio of a radiogenic or nucleogenic isotope (^{4}He, ^{21}Ne, ^{40}Ar, ^{129}Xe) to a primordial isotope of the same element, such that more degassed mantle sources develop high ratios and less degassed sources develop low ratios over time. (a) In $^{21}Ne/^{22}Ne_{(E)}$ vs $^{4}He/^{3}He$ isotope space, plume and MORB mantle sources are well-explained by differential degassing alone, with less radiogenic He and less nucleogenic Ne in plume mantle sources due to lower extents of long-term degassing of the plume source. See Moreira (2013) for a comprehensive compilation and review of He-Ne systematics in mantle-derived samples; only samples shown in other panels are shown here in He-Ne space. In (b) $^{40}Ar/^{36}Ar_{(E)}$ vs $^{4}He/^{3}He$ and (c) $^{129}Xe/^{130}Xe_{(E)}$ vs $^{4}He/^{3}He$ isotope spaces, plume mantle sources exhibit low ratios (purple fields), consistent with a less-degassed mantle source. However, among MORB mantle sources (orange fields), a wide range of $^{40}Ar/^{36}Ar_{(E)}$ and $^{129}Xe/^{130}Xe_{(E)}$ is observed with limited variation in $^{4}He/^{3}He$ and $^{21}Ne/^{22}Ne_{(E)}$. In particular, samples from the SWIR Eastern Orthogonal Supersegment are characterized by low $^{40}Ar/^{36}Ar_{(E)}$ and $^{129}Xe/^{130}Xe_{(E)}$, but He and Ne isotopic compositions similar to other MORBs (Parai et al., 2012). (d) In $^{129}Xe/^{130}Xe_{(E)}$ vs. $^{40}Ar/^{36}Ar_{(E)}$ isotope space, these low ratios are best explained by preferential incorporation of recycled atmospheric Ar and Xe, but not He or Ne, into the SWIR Eastern Orthogonal Supersegment. These systematics demonstrate that atmospheric Ar and Xe are regassed into the mantle, and that He and Ne are not sensitive tracers of recycled material.

as a potential explanation for the low $^{40}Ar/^{36}Ar$ and $^{129}Xe/^{130}Xe$ in the Eastern Orthogonal Supersegment. However, two high-^{3}He SWIR samples from 7°E most likely represent the Bouvet plume signature, and these plot with the Iceland and Samoan plume data ($^{4}He/^{3}He$, $^{21}Ne/^{22}Ne$ and $^{40}Ar/^{36}Ar$ are all unradiogenic; see Fig. 8). We also note that the Eastern Orthogonal Supersegment is geographically farther

removed from the current Bouvet plume location than the Western Orthogonal Supersegment. Thus, incorporation of less-degassed Bouvet plume material cannot explain low $^{40}Ar/^{36}Ar$ and $^{129}Xe/^{130}Xe$ paired with high $^{21}Ne/^{22}Ne$ and $^{4}He/^{3}He$ in the Eastern Orthogonal Supersegment.

Atmospheric $^{40}Ar/^{36}Ar$ and $^{129}Xe/^{130}Xe$ ratios are low compared to mantle values, and atmospheric He recycling is negligible and Ne appears not to be recycled in significant quantities (Holland and Ballentine, 2006; Sumino et al., 2010; Section 5). Thus, preferential incorporation of atmospheric Ar and Xe could explain the low SWIR Eastern Orthogonal Supersegment $^{40}Ar/^{36}Ar$ and $^{129}Xe/^{130}Xe$ ratios paired with relatively radiogenic $^{4}He/^{3}He$ and $^{21}Ne/^{22}Ne$. Parai et al. (2012) showed that there was no resolvable variation in the degree of degassing recorded in the Xe isotope systematics of the Eastern and Western Orthogonal Supersegment by comparing their slopes in $^{136}Xe/^{130}Xe$ vs. $^{129}Xe/^{130}Xe$ space. Rather, the Xe isotopic signatures of Eastern and Western Orthogonal Supersegment mantle sources could be explained by preferential regassing of atmospheric Xe into the Eastern Orthogonal Supersegment (Fig. 8). This result implies MORB mantle noble gas heterogeneity on the lengthscale of hundreds of kilometers. Parai and Mukhopadhyay (2015) further tested the hypothesis of differential regassing in the SWIR Orthogonal Supersegment using the linear least-squares mantle Xe modeling approach outlined in Section 3, and found that on average, the Eastern Orthogonal Supersegment mantle source Xe composition was best modeled with a higher proportion of regassed atmospheric Xe. Overall, continental well gases and MORBs from the SWIR provide evidence that atmospheric Ar and Xe are retained within subducting slabs beyond depths of magma generation and recycled into the deep Earth.

4.2. Recycled atmospheric xenon in the plume source: Icelandic mantle is not purely primordial

Subducted materials bearing atmosphere-derived heavy noble gases are incorporated into both the MORB mantle and the mantle source of plumes. Linear least-squares analysis (Section 3) indicates that >90% of Icelandic mantle source ^{132}Xe is derived from atmospheric recycling (Mukhopadhyay, 2012). For Rochambeau Rift samples from the Lau Basin, which are influenced by the Samoan plume, >80% of mantle source ^{132}Xe is from recycling of atmospheric Xe (Pető et al., 2013). Thus, it is clear that subducted materials cannot be exclusively re-circulated within the MORB mantle; some volatile-bearing subducted slab material must mix with mantle plumes.

A fundamental consequence of this result is that the Iceland and Samoan plume mantle sources are not purely primordial. Thus, Xe isotopes are consistent with the lithophile isotopic compositions of these samples, which necessarily reflects a mantle source that has incorporated recycled components. It is not possible to distinguish geochemically between entrainment of recycled material by upwelling plumes and incorporation of recycled slab material directly into the deep mantle source of plumes. However, the dominance of recycled atmospheric Xe in the Icelandic mantle source indicates that the bulk geochemical character of the mantle melting beneath Iceland is not that of pure primordial mantle, despite low $^{4}He/^{3}He$ ratios. The same is true of the Samoan plume mantle source sampled at the Rochambeau Rift. The fact that Xe isotopic signatures of ancient mantle heterogeneity (Mukhopadhyay, 2012; Pető et al., 2013; Section 6) are retained in the Iceland and Samoan mantle sources indicates that these mantle sources have incorporated recycled materials bearing atmospheric Xe over time without being entirely overprinted by those recycled signatures.

Low $^{4}He/^{3}He$ ratios (more commonly reported as high $^{3}He/^{4}He$ ratios) are often used as indicators of a primitive or even primordial mantle source (e.g., samples from Baffin Island and West Greenland with the lowest measured $^{4}He/^{3}He$ ratios; Rizo et al., 2016; Starkey et al., 2009; Stuart et al., 2003). Low $^{4}He/^{3}He$ values at Baffin Island have been suggested to reflect a mixture of primitive mantle with depleted mantle (Ellam and Stuart, 2004). However, the lithophile compositions of these samples have also been interpreted as representing primordial mantle (Jackson et al., 2010). Icelandic $^{4}He/^{3}He$ is among the least radiogenic measured (Hilton et al., 1999), and the Icelandic neon isotopic signature is among the most primitive measured (Mukhopadhyay, 2012; Trieloff et al., 2000). The prevalence of recycled Xe in the Iceland mantle source indicates preferential retention of atmospheric Xe relative to He and Ne in downgoing slabs. Accordingly, He and Ne isotopes do not give a full picture of mantle degassing and regassing. Therefore, helium and neon isotopic compositions should not be used to infer a pristine primordial mantle source, as these systems are not sensitive tracers of recycling.

Previous studies have noted that low $^{4}He/^{3}He$ ratios in mantle-derived basalts are associated with Nd isotopic signatures that are depleted relative to a chondritic bulk silicate Earth value (Class and Goldstein, 2005; Hart et al., 1992; Jackson et al., 2010; Jackson and Carlson, 2011; Jackson and Jellinek, 2013; Zindler and Hart, 1986). Helium-poor recycled slabs develop radiogenic $^{4}He/^{3}He$ over time, but helium concentrations in these recycled materials are extremely low compared to ambient mantle. Accordingly, mixing of ancient recycled slabs with very low concentrations of radiogenic $^{4}He/^{3}He$ into ambient mantle has a limited impact on the bulk helium isotopic composition of the resulting mantle mixture (e.g., Day and Hilton, 2011; Hanyu et al., 1999; Parai et al., 2009). Gonnermann and Mukhopadhyay (2009) demonstrated that as helium-poor degassed slabs with depleted bulk slab trace element signatures are incorporated into a relatively gas-rich plume source over time, low $^{4}He/^{3}He$ ratios may be preserved within mantle domains that are not pristine primordial reservoirs. After explicitly correcting for post- to *syn*-eruptive contamination, the Xe isotopic compositions of present-day plume mantle sources reflect a significant proportion of recycled atmospheric Xe; this observation requires that the plume mantle is not a pristine primordial reservoir and necessitates that the associated lithophile isotopic compositions not be interpreted as such.

5. Differential regassing cannot explain MORB - plume noble gas systematics

Based on noble gas elemental abundance patterns, Holland and Ballentine (2006) argued that the mantle heavy noble gas budget was dominantly derived from recycling of seawater. Holland and Ballentine (2006) further suggested that different extents of regassing (that is, injection of noble gases from surface reservoirs into mantle reservoirs) generated the observed differences between MORB and plume mantle source radiogenic heavy noble gas isotopic compositions (e.g., $^{40}Ar/^{36}Ar$ and $^{129}Xe/^{130}Xe$). On the basis of maximum measured $^{40}Ar/^{36}Ar$ and $^{129}Xe/^{130}Xe$ values in MORBs vs. plume-derived samples (Ballentine et al., 2005; Farley and Craig, 1994; Moreira et al., 1998; Trieloff et al., 2000; Trieloff et al., 2002), Holland and Ballentine (2006) argued that plume samples in general exhibited lower maximum measured $^{40}Ar/^{36}Ar$ and $^{129}Xe/^{130}Xe$ ratios than MORBs because seawater-derived heavy noble gases were preferentially incorporated into the mantle sources of plumes.

Recent determinations of mantle source compositions corrected for *syn*- to post-eruptive atmospheric contamination show that the mantle source of plumes is indeed characterized by low $^{40}Ar/^{36}Ar$ and low $^{129}Xe/^{130}Xe$ relative to the MORB mantle source (Mukhopadhyay, 2012; Parai et al., 2012; Péron et al., 2016; Pető et al., 2013; Tucker et al., 2012), as was suggested by Holland and Ballentine (2006). Close examination of He-Ne-Ar-Xe systematics between MORB and plume samples, and of Xe isotope systematics allows a critical test of the hypothesis that low $^{40}Ar/^{36}Ar$ and $^{129}Xe/^{130}Xe$ ratios in plume-derived samples reflect preferential regassing rather than differential degassing.

Mukhopadhyay (2012) presented noble gas isotopic compositions and elemental ratios from an Icelandic basalt glass (DICE; data from Mukhopadhyay, 2012; Trieloff et al., 2000) with unfractionated

radiogenic $^{4}He/^{21}Ne$ and $^{4}He/^{40}Ar^{*}$ ratios (consistent with expected mantle production ratios, indicating minimal fractionation due to magmatic degassing; Graham, 2002; Šrámek et al., 2017; Yatsevich and Honda, 1997). Mukhopadhyay (2012) compared the Iceland data with the North Atlantic popping rock sample (2ΠD43; Kunz et al., 1998; Moreira et al., 1998), which also exhibits unfractionated $^{4}He/^{21}Ne$ and $^{4}He/^{40}Ar^{*}$ ratios. In four different plots of a noble gas isotope ratio versus an elemental ratio, Mukhopadhyay (2012) plotted step-crush data for the Icelandic basalt DICE and 2ΠD43. Mixing is linear in each of these isotope ratio – element ratio plots (reproduced with additional data in Figs. 9 and 10). For each space ($^{20}Ne/^{22}Ne$ vs. $^{3}He/^{22}Ne$, $^{40}Ar/^{36}Ar$ vs. $^{3}He/^{36}Ar$, $^{40}Ar/^{36}Ar$ vs. $^{22}Ne/^{36}Ar$ and $^{129}Xe/^{130}Xe$ vs. $^{3}He/^{130}Xe$), the normalizing isotope in the x- and y-axis is the same, such that two-component mixing produces linear arrays. Step-crushing produced linear arrays reflecting atmospheric contamination of the plume mantle sources and the 2ΠD43 MORB source. Mukhopadhyay (2012) showed that the atmosphere-mantle mixing arrays for Icelandic plume mantle and the 2ΠD43 MORB source mantle were distinct slopes radiating from the atmospheric composition. The two mantle sources could not therefore be related to one another by differential regassing (Mukhopadhyay, 2012). Low $^{40}Ar/^{36}Ar$ and $^{129}Xe/^{130}Xe$ are intrinsic characteristics of the plume source mantle, and these low ratios cannot be explained by taking a mantle composition like the 2ΠD43 MORB mantle source (Moreira et al., 1998) and injecting atmospheric Ar and Xe into it (Figs. 9, 10). Step-crush data from Galapagos (Fig. 9; (Raquin and Moreira, 2009) and the Samoan plume (Figs. 9b, 10; Pető et al., 2013), plot in agreement with the Icelandic data (Mukhopadhyay, 2012) and support this conclusion for three different plume-influenced localities. Thus, preferential regassing (Holland and Ballentine, 2006) does not entirely account for plume heavy noble gas compositions. Recycling of atmospheric Ar and Xe into the mantle does occur (Section 4), but differential regassing by itself cannot explain noble gas compositional variations between plumes and MORBs.

To rule out any confounding effect due to elemental fractionation in these isotope ratio vs. element ratio plots (Figs. 9, 10), the expected effects of equilibrium and kinetic fractionation can be examined. Mukhopadhyay (2012) noted that it is not possible to explain the relationship between plume and MORB mantle sources simultaneously in all isotope ratio – element ratio spaces by starting with one reservoir and fractionating the elemental ratios by equilibrium degassing, which favors retention of the lighter element (Figs. 9, 10). Likewise, it is impossible to explain plume and MORB systematics in all spaces by starting with one reservoir and fractionating the elemental ratios by kinetic fractionation, which favors retention of the heavier element (Figs. 9, 10). Therefore, equilibrium degassing or kinetic effects that may have fractionated elemental ratios in the magmas or in the mantle (e.g., by diffusion) do not account for the observed difference in plume and MORB mantle data arrays. Rather, the atmosphere-mantle mixing arrays reflect intrinsic differences in plume and MORB mantle source compositions.

We note that the plume-influenced sample set does not reflect a single homogeneous plume end-member composition. Variation among different plume localities is evident, and may reflect heterogeneity within the plume source or variable influence of the MORB mantle at different settings (Pető et al., 2013). However, we emphasize that systematic compositional differences are evident when plume-influenced noble gas compositions are compared to those of the MORB mantle.

6. Intrinsically distinct plume mantle source Xe reflects ancient I/Xe heterogeneity

The low $^{129}Xe/^{130}Xe$ composition of the plume mantle relative to the MORB mantle is particularly notable, as the ^{129}I-^{129}Xe system was extinct ~100 Myr after the start of the Solar System. Fig. 10 shows atmosphere-mantle mixing arrays for plume-derived basalts and 2ΠD43 MORB in $^{129}Xe/^{130}Xe$ vs. $^{3}He/^{130}Xe$ space. As in the other isotope ratio

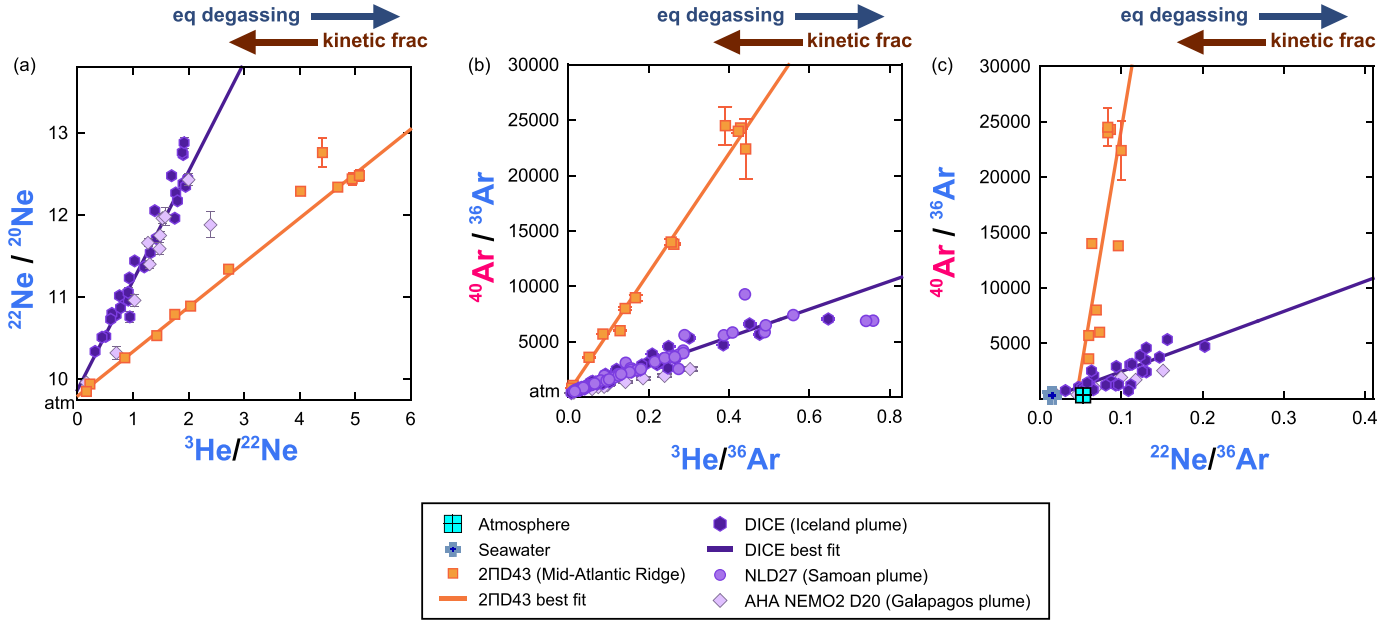

Fig. 9. Isotope-ratio vs. element-ratio plots showing distinct arrays for plume samples and MORBs. For each space, the normalizing isotope in the x- and y-axis is the same. Thus, step-crush data plotted in (a) $^{20}Ne/^{22}Ne$ vs. $^{3}He/^{22}Ne$, (b) $^{40}Ar/^{36}Ar$ vs. $^{3}He/^{36}Ar$ and (c) $^{40}Ar/^{36}Ar$ vs. $^{22}Ne/^{36}Ar$ spaces yield linear arrays reflecting atmospheric contamination of plume mantle sources (Mukhopadhyay, 2012; Pető et al., 2013; Raquin and Moreira, 2009) and the 2ΠD43 MORB source (Moreira et al., 1998). The atmosphere-mantle mixing arrays for plume mantle sources and the 2ΠD43 MORB mantle source yield distinct slopes radiating from the atmospheric composition. The plume and MORB mantle sources cannot therefore be related to one another by differential regassing. Furthermore, neither solubility-controlled equilibrium degassing (residual magma follows blue arrows) nor kinetic fractionation (residual magma follows red arrows) in the magma stage can explain plume-MORB systematics simultaneously in all three spaces: for example, if a plume-like magma experiences equilibrium degassing and develops higher $^{3}He/^{22}He$ ratios like those observed in the MORB (a), then it would also develop $^{3}He/^{36}Ar$ (b) and $^{22}Ne/^{36}Ar$ (c) ratios too high to explain the MORB composition. Likewise, if a MORB-like magma experienced kinetic fractionation due to disequilibrium degassing and developed lower $^{3}He/^{22}He$ ratios like those observed in the plume samples (a), then it would also develop $^{3}He/^{36}Ar$ (b) and $^{22}Ne/^{36}Ar$ (c) ratios too low to explain the MORB composition. This indicates that the distinct slopes are not generated by magmatic degassing, but are rather intrinsic to plume and MORB mantle sources.

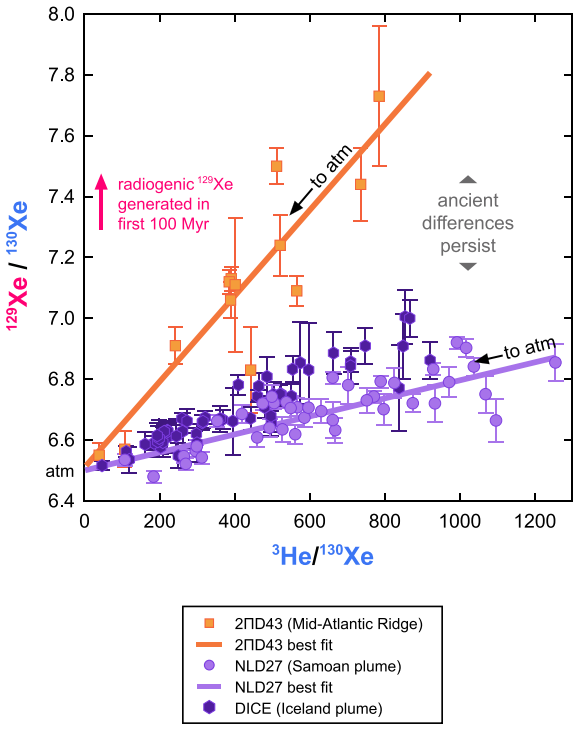

Fig. 10. ^{129}Xe/^{130}Xe vs. ^{3}He/^{130}Xe plot showing distinct arrays for plume samples and MORBs. The normalizing isotope in the x- and y-axis is the same, such that step-crush data yield linear arrays reflecting atmospheric contamination of plume mantle sources (Mukhopadhyay, 2012; Pető et al., 2013) and the 2ΠD43 MORB source (Moreira et al., 1998). The atmosphere-mantle mixing arrays for plume mantle sources and the 2ΠD43 MORB mantle source yield distinct slopes radiating from the atmospheric composition, and therefore cannot be related to one another by differential regassing. ^{129}Xe excesses are only produced during the ~100 Myr lifetime of ^{129}I, and so the distinct atmosphere-mantle mixing array for plume samples relative to the 2ΠD43 MORB sample reflect ancient I/Xe heterogeneity. This ancient ^{129}Xe signature is evident in modern basalts, and so direct mixing between MORB and plume mantle reservoirs must have been limited to preserve this heterogeneity in the mantle through 4.45 Gyr of mantle convection.

– element ratio spaces, the plume and MORB data form distinct linear arrays radiating from the atmospheric composition. The plume and MORB mantle source compositions lie along these linear arrays and cannot be related by differential regassing of atmospheric Xe (mantle sources compositions are determined based on Ne-Ar-Xe mixing systematics to correct for *syn*- to post-eruptive atmospheric contamination). Plume and MORB mantle source ^{129}Xe/^{130}Xe ratios show that the plume and MORB mantle sources *must have had distinct I/Xe ratios during the lifetime of ^{129}I.* If I/Xe variations had only developed more recently (that is, any time after 4.45 Ga), then no radiogenic signature would have developed and the mantle would only exhibit ^{129}Xe/^{130}Xe variations reflecting atmospheric regassing (that is, all mantle sources would be co-linear with the atmospheric composition).

The observation in ^{129}Xe/^{130}Xe vs. ^{3}He/^{130}Xe space that MORB and plume arrays are distinct and not collinear with the atmospheric composition is further supported by Xe isotopic systematics in plume and MORB samples. To avoid any potential elemental fractionation effects, error-weighted averages of step-crush data from plume and MORB localities are plotted in ^{129}Xe/^{136}Xe vs. ^{130}Xe/^{136}Xe isotope space (Mukhopadhyay, 2012; Parai et al., 2012; Pető et al., 2013; Tucker et al., 2012). Since ^{136}Xe is the normalizing isotope for both axes, two-component mixing generates linear arrays in this diagram. Furthermore, since all species are isotopes of Xe, elemental fractionation due to equilibrium degassing or kinetic fractionation is not a concern. Plume-MORB systematics in this isotope space re-emphasize that the plume mantle and MORB mantle sources cannot be related to one another by differential regassing (Section 5), as the mantle-derived data are not collinear with the atmospheric composition (Fig. 11).

A striking geodynamical constraint arises from the distinct arrays in ^{129}Xe/^{130}Xe vs. ^{3}He/^{130}Xe space. As the signatures preserved in these distinct mantle sources are ancient (pre-dating 4.45 Ga), the whole mantle cannot have been homogenized by 4.45 Gyr of convective mixing. If early heterogeneities in the mantle had been homogenized by mixing, then radiogenic Xe isotopic signatures from the first 100 Myr would have been mixed away into a homogeneous intermediate composition. Since distinct ancient ^{129}Xe signatures are preserved in the modern MORB source mantle and modern plume source mantle, direct mixing between the MORB and plume mantle reservoirs must have been limited over Earth history. Furthermore, recent studies have found that heterogeneous W isotopic signatures produced by decay of short-lived radioactive ^{182}Hf ($t_{1/2}$ = 8.9 Myr) are also preserved in modern basalts (Mundl et al., 2017; Rizo et al., 2016). Geodynamic models of global mantle convection must therefore meet the requirement of preserving ancient heterogeneity in the mantle: some mixing may have occurred over time, but the whole mantle could not have been homogenized at any point in Earth history.

Early separation of the plume source mantle from the MORB source is required, but heterogeneity likely exists within the plume mantle source, and certainly exists within the MORB source (Fig. 11). Plume source variations may reflect early I/Xe variations within the ancient plume source or heterogeneous incorporation of limited amounts of MORB source mantle material entrained by sinking recycled slabs. Variations among MORB sources may reflect localized plume influence in the MORB source mantle, as intermediate compositions are observed (Parai et al., 2012; Tucker et al., 2012). While mantle source compositions that are intermediate to or more extreme than those shown in Fig. 11 are likely to be found in future studies, the distinct arrays found so far require the preservation of distinct ancient reservoirs in the modern mantle.

Accretional processes may give rise to variations in the short-lived radionuclide signatures of mantle reservoirs (see Ozima et al., 1985;

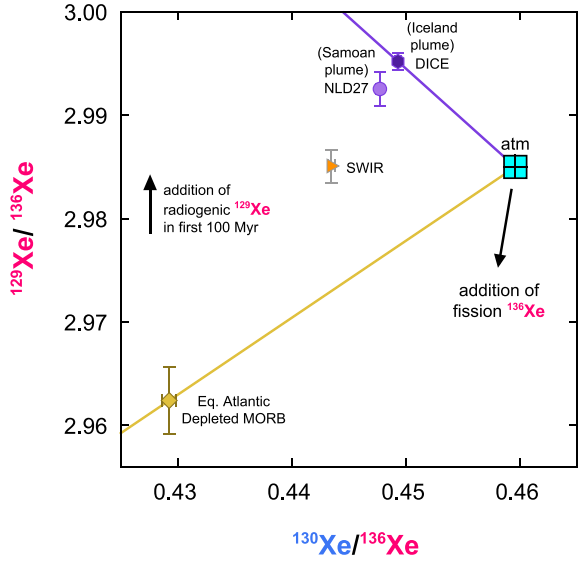

Fig. 11. Error-weighted averages of measured ^{129}Xe/^{136}Xe plotted against error-weighted average of measured ^{130}Xe/^{136}Xe for plume and MORB samples. Data from Iceland (DICE; Mukhopadhyay, 2012) and Rochambeau Rift (which samples the Samoan plume, NLD27; Pető et al., 2013) are shown with depleted equatorial Atlantic MORB (Tucker et al., 2012) and average SWIR Orthogonal Supersegment values. The atmospheric composition is indicated along with vectors representing ^{129}I decay and (Pu + U) fission. Mixing in this space is linear; MORB and plume error-weighted average compositions are not collinear with the atmospheric composition, ruling out differential regassing as the explanation for low ^{129}Xe/^{130}Xe in plume samples.

Staudacher and Allegre, 1982). Ancient I/Xe variations between mantle reservoirs may have been generated by differential early degassing of the growing Earth during the ~100 Myr lifetime of ^{129}I. In this case, I/Xe variations would be driven primarily by differential Xe loss. It is also possible that the portion of the accreting Earth that became the plume source acquired or retained less iodine than the MORB source mantle early in Earth history. Based on linear least squares analysis of mantle source compositions corrected for *syn*- to post-eruptive atmospheric contamination (Section 3), ratios of ^{129}I-produced ^{129}Xe* to ^{244}Pu fission-derived $^{136}Xe_{Pu}$ were determined for plume and MORB source mantle-derived sources (Caracausi et al., 2016; Mukhopadhyay, 2012; Parai and Mukhopadhyay, 2015; Pető et al., 2013; Tucker et al., 2012; Table 3). $^{129}Xe^*/^{136}Xe_{Pu}$ are found to be relatively low in plume mantle sources compared to MORB mantle sources (Fig. 12). If the I/Pu ratio of the whole mantle were homogeneous, then low $^{129}Xe^*/^{136}Xe_{Pu}$ ratios in the plume mantle would indicate that the lower mantle closed to catastrophic volatile loss after the MORB source mantle (Mukhopadhyay, 2012). A more physically likely explanation is that I/Pu ratios were distinct in the ancient plume and MORB sources, with lower I/Pu ratios in the ancient plume source mantle. Such a scenario could reflect either heterogeneous volatile accretion, with early accretion being volatile-poor (consistent with expected accretion of other volatiles, e.g., Morbidelli et al., 2012; Rubie et al., 2015; Schönbächler et al., 2010), or sequestration of iodine into the core due to siderophile behavior at high pressures (Armytage et al., 2013; Jackson et al., 2018). If early core-mantle differentiation generated an I-Xe signature, then we might expect a relationship between I-Xe and the short-lived Hf-W system. While the origin of ^{182}W isotope anomalies recently observed in modern basalts (Mundl et al., 2017; Rizo et al., 2016) is unclear, we suggest that measurements of ^{182}W and ^{129}Xe isotopic anomalies in the same samples would shed new light on the nature of early-formed heterogeneities lingering in the modern mantle.

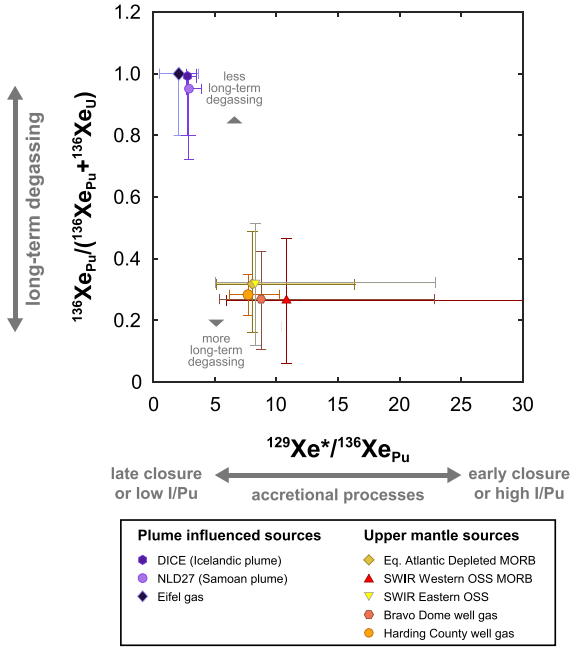

Fig. 12. Distinct radiogenic and fissiogenic Xe signatures in plume and MORB source mantle sources, after Caracausi et al. (2016). $^{129}Xe^*/^{136}Xe_{Pu}$ denotes the ratio of ^{129}Xe produced by ^{129}I decay to ^{136}Xe produced by Pu-fission Xe. Thus, variation in the x-axis reflects accretional processes on the early Earth. If the mantle had homogeneous I/Pu ratios throughout, then low $^{129}Xe^*/^{136}Xe_{Pu}$ ratios would indicate that a mantle reservoir closed (that is, ceased open system outgassing) relatively late during the lifetime of ^{129}I (a ratio of ~0 indicates closure after ^{129}I went extinct). Low $^{129}Xe^*/^{136}Xe_{Pu}$ in plume mantle sources (Caracausi et al., 2016; Mukhopadhyay, 2012; Pető et al., 2013) relative to MORB source mantle sources (Caffee et al., 1999; Holland and Ballentine, 2006; Parai et al., 2012; Tucker et al., 2012) would then suggest that the MORB source mantle closed prior to the plume source. Since this is physically unlikely, low $^{129}Xe^*/^{136}Xe_{Pu}$ in the plume source may reflect low I/Pu ratios in the ancient plume source. The y-axis is the fraction of fission-produced ^{136}Xe that is derived from ^{244}Pu-fission. Variation in the y-axis reflects the long-term degassing history of a mantle reservoir: a less-degassed reservoir would retain more of the ^{136}Xe generated by ^{244}Pu fission in the first ~500 Myr of Earth history (Table 1). Plume sources are characterized by high $^{136}Xe_{Pu}/(^{136}Xe_{Pu} + ^{136}Xe_U)$ ratios, indicating less long-term degassing than MORB source mantle sources. Plume mantle sources exhibit entirely distinct I-Pu-U-Xe signatures relative to MORB and well gas mantle sources, reflecting distinct early and long-term volatile transport histories.

7. The plume source has experienced less long-term degassing than the MORB source

Pu-fission Xe and U-fission Xe budgets shed light on the long-term processing histories of mantle sources. ^{244}Pu decays with a half-life of 80.0 Myr, such that production of any Pu-fission Xe isotope (e.g., $^{136}Xe_{Pu}$) was effectively complete at ~500 Myr (Table 1). Decay of extant ^{238}U (half-life = 4.468 Gyr) has continuously produced U-fission Xe isotopes (e.g., $^{136}Xe_U$) throughout Earth history. Degassing of mantle sources removes Xe isotopes of all origins (among fission-produced ^{136}Xe, both $^{136}Xe_{Pu}$ and $^{136}Xe_U$ are lost), but after ^{244}Pu has gone extinct, only U-fission Xe is produced in the mantle ($^{136}Xe_U$ is continuously added). A mantle source that has experienced little long-term degassing retains a relatively high proportion of Pu-fission Xe in its total fission Xe budget, whereas a mantle source that has experienced extensive long-term degassing will develop a fission Xe budget dominated by U-fission. A mantle source that has experienced no degassing is expected to develop a $^{136}Xe_{Pu}/(^{136}Xe_{Pu} + ^{136}Xe_U)$ ratio (that is, the fraction of fission ^{136}Xe that is derived from Pu-fission; see Section 3) of ~0.97 (Azbel and Tolstikhin, 1993; Tolstikhin and O'Nions, 1996). Assuming the initial mantle Xe composition was average carbonaceous chondrite (Caracausi et al., 2016), plume-influenced mantle source $^{136}Xe_{Pu}/(^{136}Xe_{Pu} + ^{136}Xe_U)$ ratios range from 0.65 to 0.97 (Fig. 12; Mukhopadhyay, 2012; Pető et al., 2013; Caracausi et al., 2016). MORB source mantle $^{136}Xe_{Pu}/(^{136}Xe_{Pu} + ^{136}Xe_U)$ ratios are generally lower (Fig. 12; Tucker et al., 2012; Parai and Mukhopadhyay, 2015) though some variability may be present (Péron and Moreira, 2018). The observed difference in plume and MORB source mantle $^{136}Xe_{Pu}/(^{136}Xe_{Pu} + ^{136}Xe_U)$ ratios shows that the plume source mantle has experienced less degassing associated with long-term mantle processing relative to the MORB source mantle. This fission Xe isotopic constraint is independent of other radiogenic noble gas systems and supports the interpretation of ^{4}He/^{3}He and ^{21}Ne/^{22}Ne systematics in plume and MORB samples as reflecting differential degassing (Fig. 8).

While variations in radiogenic and fissiogenic noble gas isotopes reflect differential degassing of the plume and MORB mantle sources, it is important to note that these two reservoirs are not simply related by different extents of degassing from a common ancient source. Rather, the signatures of long-term differential degassing are instead superimposed on ancient heterogeneities (Section 6) and extensive regassing (Section 4).

8. Summary

The origin of the reservoir supplying noble gases to plumes is fundamentally distinct from that of the MORB mantle reservoir: the two reservoirs cannot be related simply by differential degassing or incorporation of recycled atmospheric volatiles (Mukhopadhyay, 2012; Parai et al., 2012; Pető et al., 2013; Tucker et al., 2012). Through the lens of short-lived radioactive systems sensitive only to early Earth processes, we find that the plume mantle preserves an ancient signature of early differentiation. Distinct radiogenic isotope ratios from the extinct ^{129}I-^{129}Xe system are preserved in modern plume-influenced basalts and MORBs. These ancient signatures indicate that the plume source separated from the MORB source within 100 Myr of the start of the Solar System, and that the two sources have not been homogenized

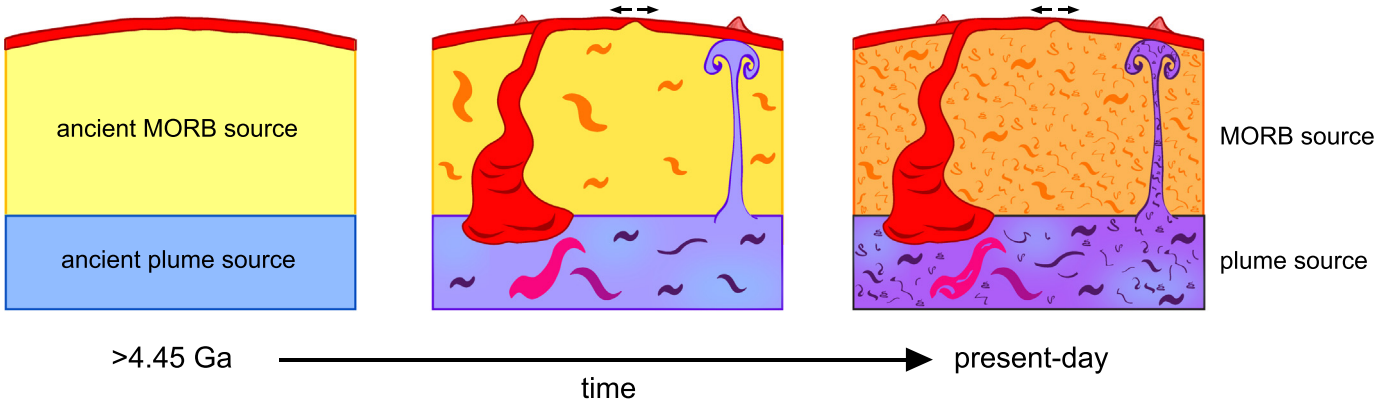

Fig. 13. Conceptual synthesis of new constraints on the nature of plume and MORB mantle sources. The plume and MORB precursor reservoirs separated prior to 4.45 Ga, during the lifetime of ^{129}I (blue and yellow reservoirs, respectively). Recycled slabs (red) were incorporated into both MORB and plume mantle sources over time, as evidenced by the dominance of regassed atmospheric Xe in the plume and MORB mantle sources (Fig. 7), though regassed Xe did not entirely overprint either mantle Xe signature. Recycled material mixed with ambient mantle and imparted bulk depleted geochemical characteristics to both the plume and MORB mantle reservoirs (yellow becoming orange; blue becoming purple in successive snapshots). Direct mixing between the two reservoirs was limited over Earth history, such that the whole mantle was never homogenized after 4.45 Ga. Faster overturn rates for the MORB source mantle resulted in a greater extent of degassing for the MORB source (Gonnermann and Mukhopadhyay, 2009). In the present-day, we observe the integrated signature of these processes: a mantle that retains ancient Xe heterogeneity, but also exhibits signatures of long-term degassing and regassing. The plume mantle source thus preserves an ancient signature and is continuously evolving.

by 4.45 Gyr of mantle convection (Caracausi et al., 2016; Mukhopadhyay, 2012; Parai et al., 2012; Pető et al., 2013; Tucker et al., 2012). Thus, direct mixing of the plume and MORB sources must have been limited over Earth history. Xe fission isotope systematics further indicate that the plume source exhibits a distinct $^{129}Xe^*/^{136}Xe_{Pu}$ signature that is low relative to the MORB source. This feature likely signifies that the plume source is characterized by a lower I/Pu than the MORB source, which may reflect preferential sequestration of I in the core, or heterogeneous accretion with early accretion being volatile-poor. Thus, Xe isotopic data indicate that the plume noble gas composition has remained intrinsically distinct from the MORB source mantle volatile budget since the early Hadean.

Examination of noble gas systems that are sensitive to long-term mantle processing reveals that mantle degassing and regassing have imprinted their own signatures on mantle noble gas budgets over time. Although noble gas isotopic differences between the MORB source and plume source cannot be explained solely by regassing of atmospheric volatiles, injection and incorporation of atmospheric heavy noble gases (Ar, Xe) into both mantle sources have occurred over Earth history. Linear least squares evaluation of the mantle source Xe compositions of plumes and MORBs indicates that mantle Xe budgets are dominated, but not entirely overprinted, by recycled atmospheric Xe. Consequently, recycled material must have been incorporated into both mantle sources over time. Because He and Ne isotopic compositions are not sensitive to incorporation of recycled material due to low overall concentrations of He and Ne in recycled material relative to ambient mantle, low $^4He/^3He$ and $^{21}Ne/^{22}Ne$ ratios in plume samples are not indicative of pristine primordial mantle. In contrast, Xe must be more efficiently retained in subducting slabs. The dominance of recycled atmospheric Xe in the plume source indicates that plume lithophile isotopic compositions cannot be interpreted to reflect pristine primordial mantle. While regassing certainly occurs, the signature of differential degassing is clear in radiogenic He and Ne isotopes, and the fission isotopes of Xe independently show that the plume mantle source has experienced less long-term degassing that the MORB source mantle.

Accordingly, the noble gas isotope systematics of plume-influenced samples provide a new portrait of the plume mantle source as a heterogeneous mixture of primordial and recycled components. The modern plume mantle preserves an ancient Xe signature of early differentiation and is continuously modified through degassing and incorporation of recycled material in association with convective processes (Fig. 13). Thus, the plume source is ancient, heterogeneous, and continuously evolving. Plumes may be related to seismically-imaged deep-seated mantle structures such as large low-velocity shear provinces (LLSVPs; e.g., Burke et al., 2008; Thorne et al., 2004; Torsvik et al., 2010; Torsvik et al., 2006). The nature of these structures is debated (see Garnero et al., 2016). If plumes are derived from LLSVPs, then the structures are at least in part ancient (predating 4.45 Ga) and long-lived.

Acknowledgments

We are grateful to David Graham and an anonymous reviewer for their constructive comments, which helped to improve the manuscript, and thank Andrew Kerr for editorial handling. This work was supported by funds provided by Washington University to RP, National Science Foundation grant OCE 0929193 to SM, a Deep Carbon Observatory postdoctoral fellowship to JMT, and MSCA IPUSS-753276 and Momentum ("Lendulet-2014") Programme grants to MKP.

References

Alexander, E.C., Lewis, R.S., Reynolds, J.H., Michel, M.C., 1971. Plutonium-244 - confirmation as an extinct radioactivity. Science 172, 837–840.
Allègre, C.J., Staudacher, T., Sarda, P., Kurz, M., 1983. Constraints on evolution of Earth's mantle from rare gas systematics. Nature 303, 762.
Allègre, C.J., Staudacher, T., Sarda, P., 1987. Rare gas systematics: formation of the atmosphere, evolution and structure of the Earth's mantle. Earth Planet. Sci. Lett. 81, 127–150.
Armytage, R.M., Jephcoat, A.P., Bouhifd, M.A., Porcelli, D., 2013. Metal–silicate partitioning of iodine at high pressures and temperatures: implications for the Earth's core and 129 Xe budgets. Earth Planet. Sci. Lett. 373, 140–149.
Azbel, I.Y., Tolstikhin, I., 1993. Accretion and early degassing of the Earth: Constraints from Pu-U-I-Xe Isotopic systematics. Meteoritics 28 (5), 609–621.
Ballentine, C.J., Marty, B., Lollar, B.S., Cassidy, M., 2005. Neon isotopes constrain convection and volatile origin in the Earth's mantle. Nature 433, 33–38.
Barfod, D.N., Ballentine, C.J., Halliday, A.N., Fitton, J.G., 1999. Noble gases in the Cameroon line and the he, Ne, and Ar isotopic compositions of high μ (HIMU) mantle. J. Geophys. Res. Solid Earth 104, 29509–29527.
Basford, J.R., Dragon, J.C., Pepin, R.O., Coscio Jr., M.R., Murthy, V.R., 1973. Krypton and xenon in lunar fines. Proceedings of the Lunar Science Conference. Geochim. Cosmochim. Acta Suppl. 4, 1915–1955.
Burke, K., Steinberger, B., Torsvik, T.H., Smethurst, M.A., 2008. Plume Gene. zones at the margins of large Low Shear Velocity Provinces on the core–mantle boundary. Earth Planet. Sci. Lett. 265, 49–60.
Caffee, M., Hudson, G., Velsko, C., Huss, G., Alexander, E., Chivas, A., 1999. Primordial noble gases from Earth's mantle: identification of a primitive volatile component. Science 285, 2115–2118.
Caracausi, A., Avice, G., Burnard, P.G., Füri, E., Marty, B., 2016. Chondritic xenon in the Earth's mantle. Nature 533, 82–85.
Castillo, P.R., 2015. The recycling of marine carbonates and sources of HIMU and FOZO Ocean island basalts. Lithos 216, 254–263.
Chase, C.G., 1981. Oceanic island Pb: two-stage histories and mantle evolution. Earth Planet. Sci. Lett. 52, 277–284.

Chauvel, C., Hofmann, A.W., Vidal, P., 1992. HIMU-EM: the French Polynesian connection. Earth Planet. Sci. Lett. 110, 99–119.
Chavrit, D., Burgess, R., Sumino, H., Teagle, D.A., Droop, G., Shimizu, A., Ballentine, C.J., 2016. The contribution of hydrothermally altered ocean crust to the mantle halogen and noble gas cycles. Geochim. Cosmochim. Acta 183, 106–124.
Class, C., Goldstein, S.L., 2005. Evolution of helium isotopes in the Earth's mantle. Nature 436, 1107–1112.
Colin, A., Moreira, M., Gautheron, C., Burnard, P., 2015. Constraints on the noble gas composition of the deep mantle by bubble-by-bubble analysis of a volcanic glass sample from Iceland. Chem. Geol. 417, 173–183.
Day, J.M., Hilton, D.R., 2011. Origin of 3 he/4 he ratios in HIMU-type basalts constrained from Canary Island lavas. Earth Planet. Sci. Lett. 305, 226–234.
Depaolo, D.J., Wasserburg, G.J., 1976. Inferences about magma sources and mantle structure from variations of Nd-143-Nd-144. Geophys. Res. Lett. 3, 743–746.
Eikenberg, J., Signer, P., Wieler, R., 1993. U-Xe, U-Kr, and U-Pb systematics for dating uranium minerals and investigations of the production of nucleogenic neon and argon. Geochim. Cosmochim. Acta 57, 1053–1069.
Eisele, J., et al., 2002. The role of sediment recycling in EM-1 inferred from Os, Pb, Hf, Nd, Sr isotope and trace element systematics of the Pitcairn hotspot. Earth Planet. Sci. Lett. 196 (3-4), 197–212.
Ellam, R., Stuart, F., 2004. Coherent He–Nd–Sr isotope trends in high 3He/4He basalts: implications for a common reservoir, mantle heterogeneity and convection. Earth Planet. Sci. Lett. 228, 511–523.
Farley, K., Craig, H., 1994. Atmospheric argon contamination of ocean island basalt olivine phenocrysts. Geochim. Cosmochim. Acta 58, 2509–2517.
Farley, K.A., Poreda, R.J., 1993. Mantle neon and atmospheric contamination. Earth Planet. Sci. Lett. 114, 325–339.
Farley, K.A., Natland, J.H., Craig, H., 1992. Binary mixing of enriched and undegassed (primitive?) mantle components (he, Sr, Nd, Pb) in Samoan lavas. Earth Planet. Sci. Lett. 111, 183–199.
Garnero, E.J., et al., 2016. Continent-sized anomalous zones with low seismic velocity at the base of Earth's mantle. Nat. Geosci. 9, 481.
Gast, P.W., Tilton, G.R., Hedge, C., 1964. Isotopic composition of lead and strontium from ascension and Gough Islands. Science 145, 1181–1185.
Geldmacher, J., Hoernle, K., Klügel, A., van den Bogaard, P., Bindeman, I., 2008. Geochemistry of a new enriched mantle type locality in the northern hemisphere: implications for the origin of the EM-I source. Earth Planet. Sci. Lett. 265, 167–182.
Gonnermann, H.M., Mukhopadhyay, S., 2009. Preserving noble gases in a convecting mantle. Nature 459, U560–U588.
Graham, D.W., 2002. Noble gas isotope geochemistry of Mid-Ocean Ridge and Ocean Island Basalts: characterization of mantle source reservoirs. Rev. Mineral. Geochem. 47, 247–317.
Graham, D.W., Humphris, S.E., Jenkins, W.J., Kurz, M.D., 1992a. Helium isotope geochemistry of some volcanic rocks from Saint-Helena. Earth Planet. Sci. Lett. 110, 121–131.
Graham, D.W., Jenkins, W.J., Schilling, J.G., Thompson, G., Kurz, M.D., Humphris, S.E., 1992b. Helium isotope geochemistry of midocean ridge basalts from the South-Atlantic. Earth Planet. Sci. Lett. 110, 133–147.
Hanan, B., Graham, D., 1996. Lead and helium isotope evidence from oceanic basalts for a common deep source of mantle plumes. Science 272 (5264), 991–995.
Hanyu, T., Kaneoka, I., 1997. The uniform and low 3He/4He ratios of HIMU basalts as evidence for their origin as recycled materials. Nature 390, 273–276.
Hanyu, T., Kaneoka, I., Nagao, K., 1999. Noble gas study of HIMU and EM Ocean island basalts in the Polynesian region. Geochim. Cosmochim. Acta 63, 1181–1201.
Hart, S.R., Hauri, E.H., Oschmann, L.A., Whitehead, J.A., 1992. Mantle plumes and entrainment - isotopic evidence. Science 256, 517–520.
Hauri, E.H., Shimizu, N., Dieu, J.J., Hart, S.R., 1993. Evidence for hotspot-related carbonatite metasomatism in the oceanic upper mantle. Nature 365, 221.
Hebeda, E.H., Schultz, L., Freundel, M., 1987. Radiogenic, fissiogenic and nucleogenic noble-gases in zircons. Earth Planet. Sci. Lett. 85, 79–90.
Heber, V.S., Baur, H., Bochsler, P., McKeegan, K.D., Neugebauer, M., Reisenfeld, D.B., Wieler, R., Wiens, R.C., 2012. Isotopic mass fractionation of solar wind: evidence from fast and slow solar wind collected by the Genesis mission. Astrophys. J. 759, 121.
Hilton, D.R., Gronvold, K., Macpherson, C.G., Castillo, P.R., 1999. Extreme He-3/He-4 ratios in Northwest Iceland: constraining the common component in mantle plumes. Earth Planet. Sci. Lett. 173, 53–60.
Hilton, D.R., Macpherson, C.G., Elliott, T.R., 2000. Helium isotope ratios in mafic phenocrysts and geothermal fluids from La Palma, the Canary Islands (Spain): implications for HIMU mantle sources. Geochim. Cosmochim. Acta 64, 2119–2132.
Hiyagon, H., Ozima, M., Marty, B., Zashu, S., Sakai, H., 1992. Noble gases in submarine glasses from mid-oceanic ridges and Loihi seamount: constraints on the early history of the Earth. Geochim. Cosmochim. Acta 56, 1301–1316.
Hofmann, A.W., White, W.M., 1982. Mantle plumes from ancient oceanic crust. Earth Planet. Sci. Lett. 57, 421–436.
Holland, G., Ballentine, C.J., 2006. Seawater subduction controls the heavy noble gas composition of the mantle. Nature 441, 186–191.
Holland, G., Cassidy, M., Ballentine, C.J., 2009. Meteorite Kr in Earth's mantle suggests a late accretionary source for the atmosphere. Science 326, 1522–1525.
Honda, M., Woodhead, J.D., 2005. A primordial solar-neon enriched component in the source of EM-I-type Ocean Island basalts from the Pitcairn Seamounts, Polynesia. Earth Planet. Sci. Lett. 236, 597–612.
Honda, M., McDougall, I., Patterson, D.B., Doulgeris, A., Clague, D.A., 1991. Possible solar noble-gas component in Hawaiian basalts. Nature 349, 149.
Hudson, G.B., Kennedy, B.M., Podosek, F.A., Hohenberg, C.M., 1989. The early solar system abundance of Pu-244 as inferred from the St. Severin chondrite. Proceedings of the 19th Lunar and Planetary Science Conference. Lunar and Planetary Institute, Houston, TX, pp. 547–557.
Jackson, M.G., Carlson, R.W., 2011. An ancient recipe for flood-basalt genesis. Nature 476, U316–U377.
Jackson, M.G., Jellinek, A.M., 2013. Major and trace element composition of the high He-3/He-4 mantle: Implications for the composition of a nonchonditic Earth. Geochem. Geophys. Geosyst. 14, 2954–2976.
Jackson, M.G., Carlson, R.W., Kurz, M.D., Kempton, P.D., Francis, D., Blusztajn, J., 2010. Evidence for the survival of the oldest terrestrial mantle reservoir. Nature 466, 853.
Jackson, C.R., Bennett, N.R., Du, Z., Cottrell, E., Fei, Y., 2018. Early episodes of high-pressure core formation preserved in plume mantle. Nature 553, 491.
Kaneoka, I., Takaoka, N., 1980. Rare gas isotopes in Hawaiian ultramafic nodules and volcanic rocks: constraint on genetic relationships. Science 208, 1366–1368.
Kaneoka, I., Takaoka, N., Clague, D.A., 1983. Noble gas systematics for coexisting glass and olivine crystals in basalts and dunite xenoliths from Loihi Seamount. Earth Planet. Sci. Lett. 66, 427–437.
Kellogg, L., Wasserburg, G., 1990. The role of plumes in mantle helium fluxes. Earth Planet. Sci. Lett. 99, 276–289.
Kendrick, M.A., Scambelluri, M., Honda, M., Phillips, D., 2011a. High abundances of noble gas and chlorine delivered to the mantle by serpentinite subduction. Nat. Geosci. 4, 807.
Kendrick, M.A., Scambelluri, M., Honda, M., Phillips, D., 2011b. High abundances of noble gas and chlorine delivered to the mantle by serpentinite subduction. Nat. Geosci. 4, 807.
Kendrick, M.A., Honda, M., Pettke, T., Scambelluri, M., Phillips, D., Giuliani, A., 2013. Subduction zone fluxes of halogens and noble gases in seafloor and forearc serpentinites. Earth Planet. Sci. Lett. 365, 86–96.
Kendrick, M.A., Scambelluri, M., Hermann, J., Padrón-Navarta, J.A., 2018. Halogens and noble gases in serpentinites and secondary peridotites: implications for seawater subduction and the origin of mantle neon. Geochim. Cosmochim. Acta 235, 285–304.
Kobayashi, M., Sumino, H., Nagao, K., Ishimaru, S., Arai, S., Yoshikawa, M., Kawamoto, T., Kumagai, Y., Kobayashi, T., Burgess, R., 2017. Slab-derived halogens and noble gases illuminate closed system processes controlling volatile element transport into the mantle wedge. Earth Planet. Sci. Lett. 457, 106–116.
Kumagai, H., Dick, H.J., Kaneoka, I., 2003. Noble gas signatures of abyssal gabbros and peridotites at an Indian Ocean core complex. Geochem. Geophys. Geosyst. 4.
Kunz, J., Staudacher, T., Allegre, C.J., 1998. Plutonium-fission xenon found in Earth's mantle. Science 280, 877–880.
Kurz, M.D., Geist, D., 1999. Dynamics of the galapagos hotspot from helium isotope geochemistry. Geochim. Cosmochim. Acta 63, 4139–4156.
Kurz, M.D., Jenkins, W.J., Schilling, J.G., Hart, S.R., 1982. Helium isotopic variations in the mantle beneath the Central-North Atlantic-Ocean. Earth Planet. Sci. Lett. 58, 1–14.
Kurz, M.D., Jenkins, W.J., Hart, S.R., Clague, D., 1983. Helium isotopic variations in volcanic rocks from Loihi Seamount and the Island of Hawaii. Earth Planet. Sci. Lett. 66, 388–406.
Kurz, M.D., Curtice, J., Fornari, D., Geist, D., Moreira, M., 2009. Primitive neon from the center of the Galapagos hotspot. Earth Planet. Sci. Lett. 286, 23–34.
Lewis, R.S., 1975. Rare-gases in separated whitlockite from St. Severin chondrite - xenon and krypton from fission extinct Pu-244. Geochim. Cosmochim. Acta 39, 417–432.
Marty, B., Tolstikhin, I., Kamensky, I.L., Nivin, V., Balaganskaya, E., Zimmermann, J.-L., 1998. Plume-derived rare gases in 380 Ma carbonatites from the Kola region (Russia) and the argon isotopic composition in the deep mantle. Earth Planet. Sci. Lett. 164, 179–192.
Matsuda, J.I., Matsubara, K., 1989. Noble gases in silica and their implication for the terrestrial “missing” Xe. Geophys. Res. Lett. 16, 81–84.
Matsuda, J.-I., Nagao, K., 1986. Noble gas abundances in a deep-sea sediment core from eastern equatorial Pacific. Geochem. J. 20, 71–80.
Matsumoto, T., Chen, Y., Matsuda, J.-I., 2001. Concomitant occurrence of primordial and recycled noble gases in the Earth's mantle. Earth Planet. Sci. Lett. 185, 35–47.
McKenzie, D., O'Nions, R.K., 1983. Mantle reservoirs and ocean island basalts. Nature 301, 229.
Morbidelli, A., Lunine, J.I., O'Brien, D.P., Raymond, S.N., Walsh, K.J., 2012. Building terrestrial planets. Annu. Rev. Earth Planet. Sci. 40.
Moreira, M., 2013. Noble gas constraints on the origin and Evolution of Earth's Volatiles. Geochem. Perspect. 2, 229–230.
Moreira, M., Charnoz, S., 2016. The origin of the neon isotopes in chondrites and on Earth. Earth Planet. Sci. Lett. 433, 249–256.
Moreira, M., Raquin, A., 2007. The origin of rare gases on Earth: the noble gas ‘subduction barrier'revisited. Compt. Rendus Geosci. 339, 937–945.
Moreira, M., Staudacher, T., Sarda, P., Schilling, J.-G., Allègre, C.J., 1995. A primitive plume neon component in MORB: the Shona ridge-anomaly, South Atlantic (51–52 S). Earth Planet. Sci. Lett. 133, 367–377.
Moreira, M., Kunz, J., Allegre, C., 1998. Rare gas systematics in popping rock: isotopic and elemental compositions in the upper mantle. Science 279, 1178–1181.
Moreira, M., Doucelance, R., Kurz, M.D., Dupré, B., Allègre, C.J., 1999. Helium and lead isotope geochemistry of the Azores Archipelago. Earth Planet. Sci. Lett. 169, 189–205.
Morgan, W.J., 1971. Convection plumes in the lower Mantle. Nature 230, 42–43.
Mukhopadhyay, S., 2012. Early differentiation and volatile accretion recorded in deep-mantle neon and xenon. Nature 486, U101–U124.
Mundl, A., Touboul, M., Jackson, M.G., Day, J.M., Kurz, M.D., Lekic, V., Helz, R.T., Walker, R.J., 2017. Tungsten-182 heterogeneity in modern ocean island basalts. Science 356, 66–69.
Nakamura, Y., Tatsumoto, M., 1988. Pb, Nd, and Sr isotopic evidence for a multicomponent source for rocks of Cook-Austral Islands and heterogeneities of mantle plumes. Geochim. Cosmochim. Acta 52, 2909–2924.
O'Nions, R.K., Hamilton, P.J., Evensen, N.M., 1977. Variations in143Nd/144Nd and87Sr/86Sr ratios in oceanic basalts. Earth Planet. Sci. Lett. 34, 13–22.

Ozima, M., Podosek, F., Igarashi, G., 1985. Terrestrial xenon isotope constraints on the early history of the Earth. Nature 315, 471.
Parai, Rita, 2014. Volatiles in the Earth and Moon: Constraints on planetary formation and evolution. Doctoral dissertation. Harvard University http://nrs.harvard.edu/urn-3:HUL.InstRepos:12271793.
Parai, R., Mukhopadhyay, S., 2015. The evolution of MORB and plume mantle volatile budgets: constraints from fission Xe isotopes in Southwest Indian Ridge basalts. Geochem. Geophys. Geosyst. 16, 719–735.
Parai, R., Mukhopadhyay, S., Lassiter, J.C., 2009. New constraints on the HIMU mantle from neon and helium isotopic compositions of basalts from the Cook-Austral Islands. Earth Planet. Sci. Lett. 277, 253–261.
Parai, R., Mukhopadhyay, S., Standish, J.J., 2012. Heterogeneous upper mantle Ne, Ar and Xe isotopic compositions and a possible Dupal noble gas signature recorded in basalts from the Southwest Indian Ridge. Earth Planet. Sci. Lett. 359, 227–239.
Pepin, R.O., 1991. On the origin and early evolution of Terrestrial Planet atmospheres and meteoritic volatiles. Icarus 92, 2–79.
Pepin, R.O., 2000. On the isotopic composition of primordial xenon in terrestrial planet atmospheres. Space Sci. Rev. 92, 371–395.
Péron, S., Moreira, M., 2018. Onset of volatile recycling into the mantle determined by xenon anomalies. Geochem. Perspect. Lett. 9, 21–25.
Péron, S., Moreira, M., Colin, A., Arbaret, L., Putlitz, B., Kurz, M.D., 2016. Neon isotopic composition of the mantle constrained by single vesicle analyses. Earth Planet. Sci. Lett. 449, 145–154.
Péron, S., Moreira, M., Putlitz, B., Kurz, M., 2017. Solar Wind Implantation Supplied Light Volatiles During the First Stage of Earth Accretion.
Péron, S., Moreira, M., Agranier, A., 2018. Origin of light noble gases (He, Ne, and Ar) on Earth: a review. Geochem. Geophys. Geosyst. 19, 979–996.
Péron, S., Moreira, M.A., Kurz, M.D., Curtice, J., Blusztajn, J.S., Putlitz, B., Wanless, V.D., Jones, M.R., Soule, S.A., Mittelstaedt, E., 2019. Noble gas systematics in new popping rocks from the Mid-Atlantic Ridge (14° N): evidence for small-scale upper mantle heterogeneities. Earth Planet. Sci. Lett. 519, 70–82.
Pető, M.K., Mukhopadhyay, S., Kelley, K.A., 2013. Heterogeneities from the first 100 million years recorded in deep mantle noble gases from the Northern Lau Back-arc Basin. Earth Planet. Sci. Lett. 369, 13–23.
Podosek, F., Honda, M., Ozima, M., 1980. Sedimentary noble gases. Geochim. Cosmochim. Acta 44, 1875–1884.
Porcelli, D., Elliott, T., 2008. The evolution of he isotopes in the convecting mantle and the preservation of high 3He/4He ratios. Earth Planet. Sci. Lett. 269, 175–185.
Poreda, R., Farley, K., 1992. Rare gases in Samoan xenoliths. Earth Planet. Sci. Lett. 113, 129–144.
Ragettli, R.A., Hebeda, E.H., Signer, P., Wieler, R., 1994. Uranium Xenon Chronology - precise determination of Lambda(SF)* Y136(SF) for Spontaneous Fission of U-238. Earth Planet. Sci. Lett. 128, 653–670.
Raquin, A., Moreira, M., 2009. Atmospheric 38 Ar/36 Ar in the mantle: implications for the nature of the terrestrial parent bodies. Earth Planet. Sci. Lett. 287, 551–558.
Raquin, A., Moreira, M.A., Guillon, F., 2008. He, Ne and Ar systematics in single vesicles: mantle isotopic ratios and origin of the air component in basaltic glasses. Earth Planet. Sci. Lett. 274, 142–150.
Richard, P., Shimizu, N., Allègre, C.J., 1976. 143Nd/146Nd, a natural tracer: an application to oceanic basalts. Earth Planet. Sci. Lett. 31, 269–278.
Rizo, H., Walker, R.J., Carlson, R.W., Horan, M.F., Mukhopadhyay, S., Manthos, V., Francis, D., Jackson, M.G., 2016. Preservation of Earth-forming events in the tungsten isotopic composition of modern flood basalts. Science 352, 809–812.
Roubinet, C., Moreira, M.A., 2018. Atmospheric noble gases in Mid-Ocean Ridge Basalts: identification of atmospheric contamination processes. Geochim. Cosmochim. Acta 222, 253–268.
Rubie, D.C., Jacobson, S.A., Morbidelli, A., O'Brien, D.P., Young, E.D., de Vries, J., Nimmo, F., Palme, H., Frost, D., 2015. Accretion and differentiation of the terrestrial planets with implications for the compositions of early-formed solar system bodies and accretion of water. Icarus 248, 89–108.
Sarda, P., Moreira, M., Staudacher, T., 1999. Argon-lead isotopic correlation in Mid-Atlantic Ridge basalts. Science 283, 666–668.
Schönbächler, M., Carlson, R., Horan, M., Mock, T., Hauri, E., 2010. Heterogeneous accretion and the moderately volatile element budget of Earth. Science 328, 884–887.
Šrámek, O., Stevens, L., McDonough, W.F., Mukhopadhyay, S., Peterson, R., 2017. Subterranean production of neutrons, ^{39}Ar and ^{21}Ne: rates and uncertainties. Geochim. Cosmochim. Acta 196, 370–387.
Starkey, N.A., Stuart, F.M., Ellam, R.M., Fitton, J.G., Basu, S., Larsen, L.M., 2009. Helium isotopes in early Iceland plume picrites: constraints on the composition of high 3 he/4 he mantle. Earth Planet. Sci. Lett. 277, 91–100.
Staudacher, T., Allegre, C.J., 1982. Terrestrial xenology. Earth Planet. Sci. Lett. 60, 389–406.
Staudacher, T., Allègre, C.J., 1988. Recycling of oceanic crust and sediments: the noble gas subduction barrier. Earth Planet. Sci. Lett. 89, 173–183.
Stroncik, N., Niedermann, S., 2016. Atmospheric contamination of the primary Ne and Ar signal in mid-ocean ridge basalts and its implications for ocean crust formation. Geochim. Cosmochim. Acta 172, 306–321.
Stuart, F.M., Lass-Evans, S., Fitton, J.G., Ellam, R.M., 2003. High ^{3}He/^{4}He ratios in picritic basalts from Baffin Island and the role of a mixed reservoir in mantle plumes. Nature 424, 57–59.
Sumino, H., Burgess, R., Mizukami, T., Wallis, S.R., Holland, G., Ballentine, C.J., 2010. Seawater-derived noble gases and halogens preserved in exhumed mantle wedge peridotite. Earth Planet. Sci. Lett. 294, 163–172.
Tatsumoto, M., 1978. Isotopic composition of lead in oceanic basalt and its implication to mantle evolution. Earth Planet. Sci. Lett. 38, 63–87.
Thorne, M.S., Garnero, E.J., Grand, S.P., 2004. Geographic correlation between hot spots and deep mantle lateral shear-wave velocity gradients. Phys. Earth Planet. Inter. 146, 47–63.
Tolstikhin, I.N., O'Nions, R.K., 1996. Some comments on isotopic structure of terrestrial xenon. Chem. Geol. 129 (3), 185–199.
Torsvik, T.H., Smethurst, M.A., Burke, K., Steinberger, B., 2006. Large igneous provinces generated from the margins of the large low-velocity provinces in the deep mantle. Geophys. J. Int. 167, 1447–1460.
Torsvik, T.H., Burke, K., Steinberger, B., Webb, S.J., Ashwal, L.D., 2010. Diamonds sampled by plumes from the core–mantle boundary. Nature 466, 352.
Trieloff, M., Kunz, J., 2005. Isotope systematics of noble gases in the Earth's mantle: possible sources of primordial isotopes and implications for mantle structure. Phys. Earth Planet. Inter. 148, 13–38.
Trieloff, M., Kunz, J., Clague, D.A., Harrison, D., Allegre, C.J., 2000. The nature of pristine noble gases in mantle plumes. Science 288, 1036–1038.
Trieloff, M., Kunz, J., Allègre, C.J., 2002. Noble gas systematics of the Réunion mantle plume source and the origin of primordial noble gases in Earth's mantle. Earth Planet. Sci. Lett. 200, 297–313.
Tucker, J.M., Mukhopadhyay, S., Schilling, J.G., 2012. The heavy noble gas composition of the depleted MORB mantle (DMM) and its implications for the preservation of heterogeneities in the mantle. Earth Planet. Sci. Lett. 355, 244–254.
Vance, D., Stone, J., O'Nions, R., 1989. He, Sr and Nd isotopes in xenoliths from Hawaii and other oceanic islands. Earth Planet. Sci. Lett. 96, 147–160.
Weaver, B.L., 1991. The origin of ocean island basalt end-member compositions: trace element and isotopic constraints. Earth Planet. Sci. Lett. 104, 381–397.
Weaver, B.L., Wood, D.A., Tarney, J., Joron, J.L., 1986. Role of subducted sediment in the genesis of ocean-island basalts: geochemical evidence from South Atlantic Ocean islands. Geology 14, 275–278.
Weiss, Y., Class, C., Goldstein, S.L., Hanyu, T., 2016. Key new pieces of the HIMU puzzle from olivines and diamond inclusions. Nature 537, 666.
Wetherill, G.W., 1953. Spontaneous fission yields from uranium and thorium. Phys. Rev. 92, 907–912.
Willbold, M., Stracke, A., 2010. Formation of enriched mantle components by recycling of upper and lower continental crust. Chem. Geol. 276, 188–197.
Williams, C.D., Mukhopadhyay, S., 2019. Capture of nebular gases during Earth's accretion is preserved in deep-mantle neon. Nature 565, 78–81.
Wilson, J.T., 1973. Mantle plumes and plate motions. Tectonophysics 19, 149–164.
Yatsevich, I., Honda, M., 1997. Production of nucleogenic neon in the Earth from natural radioactive decay. J. Geophys. Res. 102 (B5), 10291–10298.
Yokochi, R., Marty, B., 2004. A determination of the neon isotopic composition of the deep mantle. Earth Planet. Sci. Lett. 225, 77–88.
York, D., 1969. Least squares fitting of a straight line with correlated errors. Earth Planet. Sci. Lett. 5, 320.
York, D., Evensen, N.M., Martinez, M.L., Delgado, J.D., 2004. Unified equations for the slope, intercept, and standard errors of the best straight line. Am. J. Phys. 72, 367–375.
Zindler, A., Hart, S., 1986. Chemical geodynamics. Annu. Rev. Earth Planet. Sci. 14, 493–571.
Zindler, A., Hart, S.R., Frey, F.A., Jakobsson, S.P., 1979. Nd and Sr isotope ratios and rare-earth element abundances in reykjanes peninsula basalts - evidence for mantle heterogeneity beneath Iceland. Earth Planet. Sci. Lett. 45, 249–262.